

https://dspace.org/

Investigation into laser triggering of high voltages

West, Nicholas John

2006-03-23
http://hdl.handle.net/10539/276

Downloaded from a DSpace repository. https://dspace.org/

Investigation into laser triggering of high voltages

Nicholas John West

A dissertation submitted to the Faculty of Engineering and the Built Environment, University of the Witwatersrand, Johannesburg, in fulfilment of the requirements for the degree of Master of Science in Engineering.

Johannesburg, May 2005

Declaration

I declare that this dissertation is my own, unaided work, except where otherwise acknowledged. It is being submitted for the degree of Master of Science in Engineering in the University of the Witwatersrand, Johannesburg. It has not been submitted before for any degree or examination in any other university.

Signed this __ day of _____ 20__

_____

Nicholas John West.

I dedicate this document to my supervisor, Prof. I. R. Jandrell

Abstract

In this thesis, laser-triggering of spark gaps was investigated. In other words, the purpose of the project, was to ascertain what type of laser (in terms of wavelength, energy and pulse width) is the most efficient to accomplish electrical breakdown across a short spark gap. The spark gap used was set up in a coaxial geometry and the gap length was able to vary from 20 mm to 2.5 mm or less. Two lasers were used: A KrF excimer (248 nm - UV) and an Nd:YAG (1064-532-355 nm). Experiments showed that a gap of 5 mm in air and a focusing lens of 100 mm, yielded the best (widest) voltage breakdown range. It was found that the key element that will ensure electrical breakdown in a spark gap, was power density (W/cm^2). A power density of about 10 GW/cm^2 is needed to create a spark in air. In the case of the KrF laser, the voltage range was found to be 2-13 kV (216 mJ/pulse). In the case of the YAG laser operating at 1064 nm (170 mJ/pulse), the range was 600 V-13 kV and for 532 nm (40 mJ/pulse), 3 kV-13 kV. The wavelength of the laser did effect the result. For 1064 nm, breakdown in air occured at 70 mJ, whereas at 532 nm, breakdown occured at 40 mJ. For the case where the SF_6 gap was used, the range was found to be much larger than in the case of air. This can be attributed to the sensitivity of this gas to high intensity electric fields.

Acknowledgements

I would like to thank my supervisor Prof. I. R. Jandrell for his support and assistance during this project. I would also like to thank the NLC and especially Dr. Andrew Forbes, Mr. Thomas du Plooy and Mr. Henk van Wyk for their help in the laser field. At the same time, I would like to thank the staff of the GENMIN laboratories for their technical assistance.

Contents

Declaration i

Abstract iii

Acknowledgements iv

Contents v

List of Figures x

List of Tables xiv

1 Introduction 1

1.1 In general 1

1.2 Thesis plan 2

1.2.1 Chapter 2 2

1.2.2 Chapter 3 2

1.2.3 Chapter 4 2

1.2.4 Chapter 5 3

1.2.5 Chapter 6 . . . 3

1.2.6 Chapter 7 . . . 3

1.2.7 Chapter 8 . . . 4

2 Electrical breakdown in gases 5

2.1 Introduction . . . 5

2.2 The Townsend Mechanism . . . 5

2.3 The Streamer mechanism . . . 8

2.4 Ionisation methods . . . 10

2.4.1 Ionisation by collision . . . 10

2.4.2 Photoionisation . . . 11

2.4.3 Ionisation by metastable atoms . . . 11

2.4.4 Thermal ionisation . . . 13

2.5 Electronegative gases . . . 13

2.5.1 Mechanisms and applications . . . 13

2.5.2 The attachment coefficient . . . 14

2.6 Breakdown under pressurised conditions . . . 16

2.7 Time lags in electrical breakdown . . . 17

2.8 Conclusion . . . 18

3 Laser Background 20

3.1 Lasers and laser parameters . . . 20

3.1.1 Lasers in general 20
3.1.2 Laser Operation 21
3.1.3 Laser Parameters 22
3.2 Laser-induced breakdown 24
3.2.1 Calculation of laser beam intensity 25
3.3 Laser-triggered spark gaps 27
3.4 Conclusion 32

4 The impulse generator 33

4.1 Introduction 33
4.2 Impulse waveforms 33
4.2.1 Lightning impulse 35
4.2.2 Switching surge 35
4.3 Impulse generators 35
4.3.1 Impulse generator efficiency 37
4.4 Impulse generator design process 38
4.4.1 Requirements 38
4.4.2 Simulations 38
4.5 Building and testing the generator 41
4.5.1 Electrical components and connections 42
4.5.2 The spark gap 44

4.5.3 Experimental performance 45

4.6 Conclusion 47

5 Experiments with the KrF Excimer laser 48

5.1 Introduction 48

5.2 The KrF laser and equipment set up 48

5.3 Results obtained from the KrF laser 52

5.3.1 Voltage withstand levels 53

5.3.2 Laser-induced breakdown results 54

5.3.3 Pre-breakdown phenomena 57

5.3.4 Beam quality improvement 59

5.4 Conclusion 61

6 Experiments with the Nd:YAG laser 62

6.1 Introduction 62

6.2 The Nd:YAG laser 62

6.3 Laser breakdown experiments 66

6.3.1 Experiment at 1064 nm (near infrared) 66

6.3.2 Experiments at 532 nm (green light) 67

6.3.3 Experiments at 355 nm (Ultraviolet) 71

6.4 Conclusion 71

7 Laser breakdown in sulphur hexafluride (SF_6) 73

7.1 Introduction 73

7.2 The spark gap used 74

7.3 Breakdown experiments 75

7.4 Conclusion 78

8 The summing up **79**

References **83**

9 Appendix **85**

9.1 Appendix A: Impulse generator model evaluation 85

9.2 Appendix B: Impulse generator experimental results 98

9.3 Appendix C: Pre-breakdown phenomena measurements 102

9.4 Appendix D: The engineering drawing 103

List of Figures

2.1 Townsend mechanism [1] 6

2.2 Field distortion caused by electron avalanche [1] 8

2.3 Breakdown variation with respect to pd 17

3.1 Operation of a laser 21

3.2 Some common modes for lasers 24

3.3 Definition of a FWHM pulse 26

3.4 Operation of the trigatron 28

3.5 The field distortion gap 28

3.6 Perpendicular spark gap arrangement 29

3.7 Coaxial spark gap arrangement 29

3.8 Absorption spectrum of SF_6 31

4.1 Impulse waveform definition 34

4.2 Impulse generator circuit 36

4.3 Marx impulse generator circuit 37

4.4 Simulink impulse generator model 38

4.5 Impulse waveform for a 2 kV charging voltage 41

4.6 Front and side view of the bracket used to mount the diode and current limiting resistor 42

4.7 The charging circuit of the impulse generator 43

4.8 Front and side view of the insulating bushing 44

4.9 Bushing mounted on impulse generator 44

4.10 Coaxial spark gap arrangement 45

4.11 Output waveform for a 900 V charging voltage 46

4.12 Output waveform for a 900 V charging voltage 47

5.1 KrF laser set up at the CSIR 49

5.2 Beam shape of the KrF laser 49

5.3 Energy meter used 50

5.4 PhotoDiode used 50

5.5 PhotoDiode used 51

5.6 Optics setup for KrF laser 51

5.7 Spot size and shape after focusing 56

5.8 Plots of the input and output voltages for thee different gap lengths 57

5.9 Plot of the prebreakdown impulse for a charging voltage of 800 V 58

5.10 Creation of space charge between a point and a plain 59

5.11 Reconstruction of laser beam by using a lens-pinhole combination 60

5.12 Use of mirrors to create a larger laser beam profile 61

5.13 Burn patterns produced by excimer with multiple mirrors 61

6.1 The Nd:YAG laser used in the experiments 63

6.2 The Nd:YAG laser pulse obtained 65

6.3 Burn pattern of YAG laser 65

6.4 Burn pattern of YAG laser at 532 nm 68

6.5 Variation of breakdown voltage as laser energy is altered 70

6.6 Variation of laser energy with varying Q-switch value 70

7.1 A simple drawing of the SF_6 spark gap 74

7.2 Plot of breakdown voltage in SF_6 vs. spark gap pressure 77

7.3 Comparing the breakdown voltages obtained from Paschen Curve with the laser-triggered voltages 77

9.1 Impulse waveform for charging voltage of 1 kV 85

9.2 Impulse waveform for charging voltage of 2 kV 86

9.3 Impulse waveform for charging voltage of 3 kV 86

9.4 Impulse waveform for charging voltage of 4 kV 87

9.5 Impulse waveform for charging voltage of 5 kV 87

9.6 Impulse waveform for charging voltage of 6 kV 88

9.7 Impulse waveform for charging voltage of 7 kV 88

9.8 Impulse waveform for charging voltage of 8 kV 89

9.9 Impulse waveform for charging voltage of 9 kV 89

9.10 Impulse waveform for charging voltage of 10 kV 90

9.11 Impulse waveform for charging voltage of 11 kV 90

9.12 Impulse waveform for charging voltage of 12 kV 91

9.13 Impulse waveform for charging voltage of 13 kV 91

9.14 Impulse waveform for charging voltage of 14 kV 92

9.15 Impulse waveform for charging voltage of 15 kV 92

9.16 Impulse waveform for charging voltage of 16 kV 93

9.17 Impulse waveform for charging voltage of 17 kV 93

9.18 Impulse waveform for charging voltage of 18 kV 94

9.19 Impulse waveform for charging voltage of 19 kV 94

9.20 Impulse waveform for charging voltage of 20 kV 95

9.21 Experimentally obtained impulse waveform for 0.9 kV charging voltage 98

9.22 Experimentally obtained impulse waveform for 2.3 kV charging voltage 99

9.23 Experimentally obtained impulse waveform for 3 kV charging voltage 99

9.24 Experimentally obtained impulse waveform for 4.1 kV charging voltage 100

9.25 Experimentally obtained impulse waveform for 5.5 kV charging voltage 100

9.26 Experimentally obtained impulse waveform for 6 kV charging voltage 101

9.27 Experimental data obtained for pre-breakdown phenomena . . . 102

9.28 Experimental data obtained for pre-breakdown phenomena . . . 103

List of Tables

2.1 The electromagnetic spectrum 12

2.2 Minimum breakdown voltages for some gases 17

4.1 Experimental results obtained from the impulse generator 46

5.1 Maximum withstand voltages for various gap sizes 53

5.2 Inital laser-induced breakdown results 54

6.1 Calibration table for the energy meter filter at 1064 nm 64

6.2 Breakdown results for 1064 nm 66

6.3 Laser-induced breakdown voltages 69

Chapter 1

Introduction

1.1 In general

In high voltage engineering, one of the most important tasks one has to perform, is the triggering of high voltages. To do this, a form of triggered spark gap is used. These devices can either be of a purely mechanical nature, or they may be more intricate. The triggered spark gap that is be far one of the most commonly used ways of triggering high voltages is the trigatron. One other very important aspect in any high voltage application, is timing. It is important to know precisely when certain events happen and how long they take to happen. In the case of triggered spark gaps, the ultimate goal is to time the breakdown process accurately, repeatable and efficiently. A good example is the SABS IEC 61643-1 document. According to this standard, surge protection devices (SPDs) are to be tested by superimposing a voltage impulse at a very specific point on the 50 Hz mains waveform. The reason why conventional spark gaps are not able to time the electrical breakdown accurately is because of the statistical time lag, that is the time taken for an electron to became available and start an electrical avalanche across the gap. This problem can be eliminated by providing the seed electrons by say irradiating the cathode with ultraviolet (UV) light. Another way of doing this is by firing a high energy laser beam into the gap and causing ionization of the gas. In this document there will be a discussion of the principles of electrical breakdown in gases. Following this, there will be a section on lasers and laser triggering of spark gaps. The design, building and testing of the simple impulse generator

that was used will be presented. Finally, an overview of the experiments and a discussion of results obtained will be presented.

1.2 Thesis plan

1.2.1 Chapter 2

In this chapter, the focus will be on some high voltage engineering background. In other words, the various breakdown mechanisms will be discussed. These will include the Townsend, Streamer and Leader processes. At the same time, the various ionisation processes that can lead to electrical breakdown will be discussed. These processes include ionisation by collision, photoionisation, ionisation from interaction with metastable atoms and thermal ionisation. Also the case of electronegative gases will be discussed.

1.2.2 Chapter 3

Following the discussion on electrical breakdown, some laser-related issued will be presented. The basic anatomy of a laser will be discussed. This will include the basic building blocks of a laser, they types of laser and some of their applications. Following this, the various parameters of a laser will be presented, namely beam size, fluence, intensity and pulse width. At the same time, an overview of the process of laser-triggering of spark gaps will be presented.

1.2.3 Chapter 4

This chapter contains an overview of the design process of the simple impulse generator that was constructed and that was used in the experiments. This generator was used to supply the voltage to be broken down by means of the laser. A brief introduction to impulse generators will be presented, followed by the design process and the final results. These results include theoretical evaluations of waveshape and efficiency. At the same time, the results obtained

from testing the generator will be presented.

1.2.4 Chapter 5

The following chapters deal with the experiments performed using the two lasers that were available at the National Laser Centre (NLC) of the CSIR. This chapter describes the setup, operation and results obtained with the KrF Excimer laser operating at 248 nm (UV range). A coaxial spark gap was used. The experiments were conducted primarily in air at atmospheric pressure and room temperature.

1.2.5 Chapter 6

In this chapter, laser induced experiments are described using an Nd:YAG laser located at the National Laser Centre in Preotoria. The laser was able to output laser light at three different wavelengths: 1064 nm (infrared), 532 nm (green) and 355 nm (ultraviolet). The laser beam had a gaussian profile. The maximum energy output of the laser was about 170 mJ per 8-10 ns pulse. Laser breakdown experiments were conducted at all three wavelengths and the results obtained are discussed and compared with those obtained in the previous chapter.

1.2.6 Chapter 7

In chapter 7, the KrF laser is revisited. This time, a spark gap mounted in an airtight container was used. The gap atmosphere was chosen to be sulphur hexafluoride (SF_6) at various pressures and room temperature. The design of the container in question is presented. The laser breakdown experiments are described and the results are discussed.

1.2.7 Chapter 8

Finally, in this chapter, the overall conclusions are presented and some recommendations for future research are presented.

Chapter 2

Electrical breakdown in gases

2.1 Introduction

High voltages are present in nearly all aspects of everyday life. They are primarily used as a means of generating and distributing electrical power. High voltages are also widely used during laboratory tests for various devices such as surge arresters. This is because one of the most common natural forms of high voltages is lighting. Lightning affects devices such as SPDs and in many cases, poses a threat to human and animal life. The process of electrical breakdown is complicated and they are many theories that are used to describe the phenomenon. The two main mechanisms are the leader and streamer process. The leader mechanism is used to explain breakdown over long gaps (gaps greater than about 20 cm). The leader mechanisms is the process that describes the formation of lightning. The streamer mechanism is used to describe breakdown in short gaps (gaps in the order of a couple of centimetres).

2.2 The Townsend Mechanism

The Townsend mechanism is the simplest model that is used to describe electrical breakdown across a gap. The model in essence describes ionization by electron collision (between atoms and molecules in the gas and collision with the surface of the electrodes) [1].

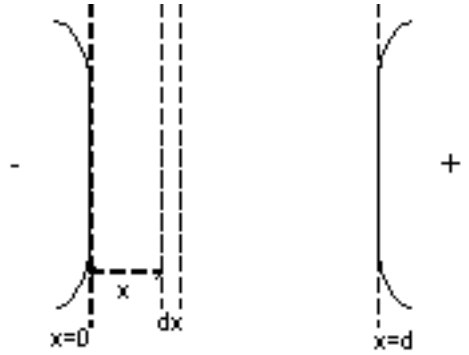


Figure 2.1: Townsend mechanism [1]

The starting point for this model is to assume two electrodes (an anode and a cathode) that set up a high electric field as can be seen in *figure 2.1.*

The gap distance is d. The model assumes that there are N_0 free electrons at the cathode. These free electrons start a series of collisions and at distance from the cathode, the electron number has increased to N. An increase in distance dx will produce an increase in electron numbers of $dN = \alpha dx$. Integration of this relationship across the gap gives the following relationship:

$$N = N_0 e^{\alpha d} \tag{2.1}$$

This Shows that the initial free electrons start an avalanche (through collision) that expands exponentially across the gap. The quantity is known as the first ionization coefficient. It is defined as the number of electrons produced by an electron collision per unit length of path in the direction of the field.

Generation of free electrons through electron collision with gas atoms and molecules is not the only process that happens in the gas. At the same time, electrons are emitted through impact with the electrode surface (secondary emission). Assuming that $\alpha N dx$ electrons are emitted by the primary ionization process, then $\omega N dx$ electrons are emitted from the cathode. These electrons are emitted due to the impact of the much heavier positive ions that are created by the electron collision process. The total number of electrons

emitted from the cathode is then:
$N_0{}' = N_0 + \int_0^d \omega N dx$. At the same time, it is known that $N = N_0{}' e^{\alpha d}$. Therefore, $N_0{}' = N_0 + \int_0^d \omega N_0{}' e^{\alpha x} dx = N_0 + \frac{\omega}{\alpha} N_0{}' \left[e^{\alpha d} - 1\right] \Rightarrow N_0 = N_0{}' \left\{1 - \frac{\omega}{\alpha}\left[e^{\alpha d} - 1\right]\right\}$
From this relation it can be seen that the total number of electrons arriving at the anode is therefore:

$$N_a = N_0{}' e^{\alpha d} = N_0 \frac{e^{\alpha} d}{\left\{1 - \left(\frac{\omega}{\alpha}\right)\left[e^{\alpha d} - 1\right]\right\}} \tag{2.2}$$

The term $\frac{\omega}{\alpha}$ is known as the second ionisation coefficient γ. This number expresses the number of electrons emitted from the cathode per incident ion [2]. It can be also seen that the number of electron charges arriving at the anode per unit time (in other words the current detected by the external circuit) can be written as:

$$I = eN_d = I_0 \frac{e^{\alpha d}}{1 - \gamma\left(e^{\alpha d} - 1\right)} \tag{2.3}$$

As the voltage (and hence the field) increases, the term $e^{\alpha d}$ increases until $\gamma e^{\alpha d} \rightarrow 0$.At this point, the denominator tends to zero and therefore, the current tends to infinity [3]. This is the condition for which we get electrical breakdown. In general terms, the Townsend criterion for breakdown can be expressed as:

$$\left(\gamma e^{\alpha d} - 1\right) = 1 \tag{2.4}$$

The Townsend mechanism is the simplest theory that describes electrical breakdown across a gap. It is interesting to state that for both the first and second ionisation coefficients (α and γ respectively) it has been found experimentally that they are dependent on the ratio $\frac{E}{p}$ where E and p are the electric field and pressure of the gas respectively. It has been found that the following relationships exist [2]:

$$\frac{\alpha}{p} = f\left(\frac{E}{p}\right) \tag{2.5}$$

$$\gamma = g\left(\frac{E}{p}\right) \tag{2.6}$$

where f and g are two arbitrary functions

When a high intensity laser beam is focused in the region of a spark gap (between the two electrodes), the following two event occur: Due to the high photon energy, the phenomenon of photoionisation occurs. This means that there is an abundance of free electrons at the focal point of the beam. At the same time, a very high local electric field is developed. The fact that a large number of free electrons are available, means that that more electron collisions can occur thus generating a large electron avalanche.

2.3 The Streamer mechanism

The Townsend mechanism is a very simple way of describing the breakdown process. It is unable, though, to explain phenomena like the irregular and random formation of a discharge in long gaps. That is why the streamer (or Kanal) processes is used. In essence, the streamer mechanism describes the development of a spark from a single electron avalanche. This is because, as the avalanche progresses and grows across the gap, a space charge is formed at the head of the electron cloud as can be seen in *figure 2.2*.

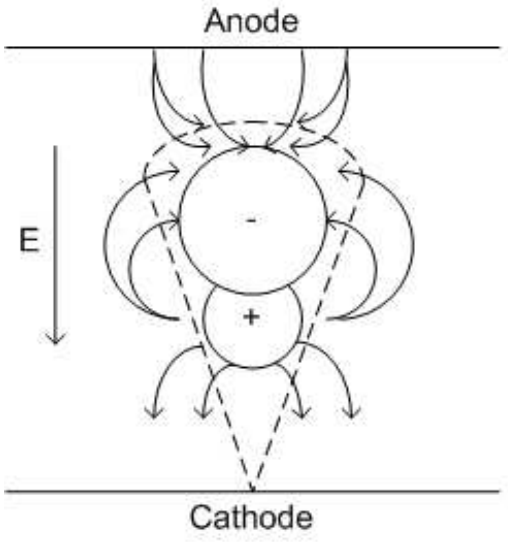


Figure 2.2: Field distortion caused by electron avalanche [1]

The result of this space charge, is the conversion of the electron avalanche into what is known as a plasma streamer. There are two main features that are

related to the streamer process. The first one is that there is a large amount of photo-ionisation present. In essence, it can be thought that the avalanche emits high energy photons from the head of the process.These photons are absorbed not too far away from the ion space charge. The newly created electron in their turn contribute to the production of more photons and so the process continues. The second point is that there is a localised enhancement of the electric field between the two electrodes. This is due to the space charge that has been formed again at the head of the streamer[1, 3]. The approximate value of the space charge field can be evaluated by assuming that the total charge Q is contained within a sphere of radius r at the head of the avalanche. The charge Q is in Coulombs (C) and the radius r is in meters (m). It is known that the electric field is given by $E_r = k\frac{Q}{r^2}$ where $k = \frac{1}{4\pi r^2}$. At the same time, the charge Q can be expressed as $Q = Ne$ where N is the number of ions per unit volume and e is the electron charge. From this information the field equation can be rewritten as:

$$E_r = \frac{(4/3\pi r^3)Ne}{4\pi\epsilon_0 r^2} \Rightarrow E_r = \frac{rNe}{3\epsilon_0} \tag{2.7}$$

As the avalanche moves forward a distance dx, the number of electrons produced will be $\alpha e^{\alpha x}dx$. This means that N can be written as $N = \frac{\alpha e^{\alpha x}dx}{\pi r^2 dx}$ (assuming a cylindrical volume). Therefore $E_r = \frac{\alpha e^{\alpha x}}{3\epsilon_0 \pi r}e$. The radius r can be obtained by considering the diffusion expression which is $r = \sqrt{2Dt}$ where D is the diffusion coefficient and $t = x/u_a$. u_a is the speed with which the avalanche progressed across the gap. Combining the above equations, the electric field due to the space charge can be expressed as:

$$E_r = \frac{\alpha e^{\alpha x}e}{3\epsilon_0 \pi\sqrt{2D\frac{x}{u_a}}} \tag{2.8}$$

With the streamer mechanism, a criterion exists that explains the transition from an electron avalanche to a streamer. This criterion is that $E = kE_r$ where $k \approx 1$. In other words, an electron avalanche develops into a streamer when the field at the head of the avalanche is approximately equal to the total electric field applied between the electrodes.

The strength of the streamer mechanism lies in the fact that it is able to explain breakdown in non-uniform fields such as point-to-plane or point-to-point gaps. It fails though to explain the breakdown process in long gaps. That is why the leader mechanism was developed [4].

2.4 Ionisation methods

As mentioned above, the key process that allows electrical breakdown to occur, is ionisation. Ionisation can happen in many different ways. Irrespective of the mechanism though, as the name implies, ionisation is the production of ions. Ions are produced when electrons are stripped from neutral atoms or molecules. In essence there are four main mechanisms that enable ionisation to take place. These are:

1. Ionisation by collision
2. Photoionisation
3. Ionisation by metastable atoms
4. Thermal ionisation

In the case of laser triggering of spark gaps, the ionisation forms that become

2.4.1 Ionisation by collision

This is the most common form of ionisation. It is the principle of the Townsend ionisation process. Electrons with high enough energies are able to strip other electrons off neutral atoms. The number of electrons produced through collision depends on the type of atoms or molecules and the mean free path between them. It also depends on the average velocity of the electrons. This process is very important when the electric field is very high. This is because electrons do not lose too much energy through collisions, but they are able to build up their kinetic energy supplied by the electric field. To cause ionisation through

impact, the transferred energy must be equal to, or greater than the ionisation potential of the molecule. For example, the ionisation energy of an Oxygen atom is 13.6 eV, whereas for Nitrogen it is 14.5 eV. The transferred energy is closely related to the mean free path λ between atoms ($\delta W = e\lambda$). It must be mentioned though, that ionisation by electron collision is a probabilistic phenomenon. In some cases ionisation does not take place even though the colliding electron my have the required energy [2].

Another important factor that determines how easy a gas is ionised, is the ionisation cross section of the molecules or atoms in question.

2.4.2 Photoionisation

In many cases, a low energy electron may on collsion with a neutral gas atom exite it to a higher energy state. When the atom returs to is relaxed state, a photon is emitted. This photon may be able to ionise another atom whose ionisation energy is lower than the photon energy. The process can be symbolically written as $A + hf = A^* + e$, where A and A^* represent the neutral and exited atom of the gas. hf is the photon energy. As mentioned, for photoionisation to occur, the photon energy hf must be greater than the atom ionisation energy. The photon energy depends on the photon wavelength. The shorter the wavelength, the higher the photon energy. The electromagnetic spectrum can be seen below together with the associated photon energies in *table 2.1.* Only part of the spectrum is visible. It is the electromagnetic waves from 400 to 700 nm [5]

This means that the breakdown process can be assisted by irradiating the electrodes with a light source whose photons have a high energy. The commonest way is to user a source of Ultraviolet light.

2.4.3 Ionisation by metastable atoms

Another ionisation process, is ionisation due to metastable atoms. Metastable atoms are atoms whose lifetime in the exited state can last up to a couple

Region	Wavelength	Frequency (Hz)	Energy (eV)
Radio	> 0.1 m	< 3×10^{9}	< 10 μeV
Microwave	0.1 m – 100 μm	3×10^{9} - 3×10^{12}	10 μeV – 10 meV
Infrared	100 μm – 700 nm	3×10^{12} - 4.3×10^{14}	10 meV – 2eV
Visible	700 nm – 400 nm	4.3×10^{14} - 7.5×10^{14}	2eV – 3eV
Ultraviolet	400 nm – 1 nm	7.5×10^{14} - 3×10^{17}	3eV – 10 keV
X-Rays	1 nm – 10 pm	3×10^{17} - 3×10^{19}	10 keV – 100 keV
Gamma Rays	< 10 pm	> 3×10^{19}	> 100 keV

Table 2.1: The electromagnetic spectrum

of seconds. The result of this is that their energy is high enough to cause ionisation of neutral atoms. Depending on the metastable energy (V_m), The following situations can arise:

1. If $V_m > V_i$ (where V_m refers to atom A^m and V_i refers to atom B). In this case, the process can be written as

$$A^m + B \rightarrow A^+ + B + e \tag{2.9}$$

2. If $V_m > V_i$ (where V_m refers to atom A^m and V_i refers to atom B). The process is be expressed as

$$A^m + B \rightarrow A + B^* + e \tag{2.10}$$

3. In the case where $2V_m > V_i$ (where both V_m refers to A^m and V_i refer to atom A). The reaction that happens can be written as

$$2A^m \rightarrow A^+ + A + e + KE \tag{2.11}$$

4. Finally, in some cases the following may occur:

$$A^m + 2A \rightarrow A_2^* + A \tag{2.12}$$

and

$$A_2^* \rightarrow A + A + hf \tag{2.13}$$

The photon emitted does not usually have enough energy to cause ionisation in a gas. It way though induce electrons to be emitted form the cathode.

It is interesting to note that ionisation by metastable atoms is more effective in gas mixtures.

2.4.4 Thermal ionisation

Thermal ionisation is a form of ionisation that is not often observed. The basic principle is that when the temperature of a gas is sufficiently high, the vibration of the molecules become very significant. These vibrations can result in ionisation due to molecules colliding with each other. Thermal ionisation becomes significant at temperatures above 1000 K.

2.5 Electronegative gases

2.5.1 Mechanisms and applications

There are a certain category of gases that have the ability to readily acquire electrons from stable negative ions. These are known as electronegative gases. These gases lack one or two electrons in their outer shells. Such gases include the halogens (F, Cl, Br, I, At) and gases such as oxygen (O) or sulphur (S).

A very important parameter associated with electronegative gases, is their electron affinity. This quantity is defined as the change in energy that occurs when en electron is attached to the gaseous form of the atom. For example, the electron affinity for Hydrogen is $-72\ kJ/mole$. where as the electron affinity for Fluorine is $-330\ kJ/mole$.

Electronegative gases are used quite often as insulators. The most potent electronegative gas used in this capacity if sulphur hexafluride (SF_6). As a gas, SF_6, has an excellent dielectric strength. It is about 2.5 times that of air. It also has the ability (as an electronegative gas) to quench arcs very effectively. The gas is obtained from molten sulphur and gaseous fluorine. It is refined to 99.9% purity [6]. Electron detachment is the main mechanism associated

with electronegative gases. Abdel-Salam and Turkey in 1988[1] ascribed the detachment process to the following events [4]:

1. Photodetachment. In this situation, a quantum of energy (in the form of a photon) is absorbed by the negative ion. This can be written as follows:
$$A^- + hf \rightleftharpoons A + e \tag{2.14}$$

2. Ion collision with fast atoms:
$$A^- + A \rightleftharpoons 2A + e \tag{2.15}$$

3. Collision and association with a neutral atom. This process normally leads to the loss of an excessive electron.
$$A^- + B \rightleftharpoons AB + e \tag{2.16}$$

4. A molecular negative ion may at some point collide with a fast excited atom. This results in the negative ion becoming excited:
$$A_2^- + B^* \rightleftharpoons A_2^* + e \tag{2.17}$$

5. Finally, recombination can occur between negative and positive ions of atoms. The result is the formation of a diatomic molecule:
$$A^- + B^- \rightleftharpoons AB^+ + e \tag{2.18}$$

2.5.2 The attachment coefficient

In analogy to the first ionisation coefficient (α) that expressed the number of electrons released for per electron collision, a similar coefficient exists for the case of electronegative gases. This coefficient expresses the number of attachments produced in a path of a single electron travelling a distance of 10 mm in the direction of the field. In this case, the electron current will decrease in accordance with the relationship:
$$I_{loss} = I_0 e^{-\eta d} \tag{2.19}$$

[1]M. Abdel-Salam, A. Turkey, (1988), IEEE Trans., IA-24: 1031

where d is the gap distance.

Considering the two basic mechanisms (electron multiplication through electron collision and electron attachment) one can say that the two processes complement each other. Therefore, breakdown will occur if the number of electrons produced is more than the number of electrons attached. One can express this mathematically as follows:

Let the number of electrons produced via electron collision by $dn_c = n\alpha dx$ (From Townsend). At the same time, let n_a be the number of electrons attachted by the electronegative gas. In other words, $dn_a = -n\eta dx$. From this we can calculate the number of electrons that are still free in the gas. This number can be given by: $dn = dn_c + dna = n(\alpha - \eta)dx$. By Integration (from $x = 0$ to $x = d$) the number at any point in the gap can be expressed as

$$n = n_0 e^{(\alpha-\eta)} d \tag{2.20}$$

where n_0 is the number of electrons at the cathode. The total current that is observed, has two components: One resulting from ionisation be collision and one resulting from deionisation by attachment. The latter can be expressed as $dn_{neg} = n\eta dx = n_0\eta e^{(\alpha-\eta)dx}$. By integrating across the gap,

$$n_{neg} = \frac{n_0\eta}{\alpha - \eta}[e^{(\alpha-\eta)d} - 1] \tag{2.21}$$

The overall current can be expressed as follows:

$$\frac{n + n_{neg}}{n_0} = \frac{\alpha}{\alpha - \eta} e^{(\alpha-\eta)d} - \frac{\eta}{\alpha - \eta} \tag{2.22}$$

The final equation is therefore:

$$I = I_0[\frac{\alpha}{\alpha - \eta} e^{(\alpha-\eta)d} - \frac{\eta}{\alpha - \eta}] \tag{2.23}$$

2.6 Breakdown under pressurised conditions

In gases, as it is expected, breakdown depends heavily on parameters such as pressure, temperature and electric field strength. If any of these parameters change, the breakdown strength of the gas is expected to change. This relationships that describe this phenomenon were developed by Paschen.

By considering the equations (2.4), (2.5) and $E = \frac{V}{d}$, it can be seen that:

$$\gamma(e^{\alpha d} - 1) = 1 \Rightarrow g\left(\frac{V}{pd}\right)\left(e^{pdf\left(\frac{V}{pd}\right)} - 1\right) = 1$$

From this equation it can be seen that the breakdown voltage depends on the gap separation d and the gas pressure p. This relationship also applies to the case of electronegative gases. In general, Paschen's law can be expressed as

$$V = f(pd) \tag{2.24}$$

This relationship can be represeneted by the graph in *figure 2.3*. From this plot, it can be seen that for a constant gap spacing, as the pressure increases (starting from vacuum) the breakdown voltage decreases unitl it reaches a minumum value. Then the breakdown voltage increases with increasing pressure. This can be explained by considering the mean free path between the atoms that comprise the gas. Initially, because of vacuum conditions, the brealkdown voltage is high (no electrons can be produced via collisions or other processes). As gas atoms are injected into the system, free electrons become easier to produce and therefore, the the breakdown voltage decreases. At some point though, the mean free path starts becoming too short thus hindering the electron multiplication process. In *table 2.2*, some miniumm breakdown voltages for various gases can be seen.

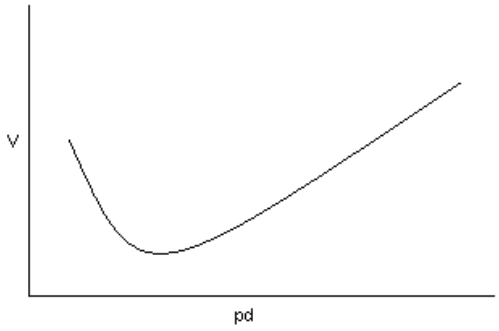


Figure 2.3: Breakdown variation with respect to pd

Gas	pd (min) [bar mm]	Vb (min) [V]
Air	0.0073	352
N_2	0.0085	240
SF_6	0.0034	507
CO_2	0.0075	420
Ne	0.0526	245

Table 2.2: Minimum breakdown voltages for some gases

2.7 Time lags in electrical breakdown

One of the most important parameters in electrical breakdown situations, is time. In some applications, it is very important to know when exactly breakdown phenomena take place. If a step voltage is applied to a gap, then there will be a finite time before the gap actually breaks down. This time t is made up of two components. These are the formative (t_f) and the statistical (t_s) time lags.

The statistical time lag is the most problematic of the two. It is the time taken for a free electron to become available at the cathode and start the electron avalanche that will lead to electrical breakdown across the gap. As the name implies, this time lag is variable. On average it is about $0.1ms$ [7]. The statistical time lag can be controlled (or eliminated completely) by providing the free electrodes required. This can be done by irradiating the cathode with ultraviolet (UV) light. Because of the short wavelength, electrons become available through photoionisation.

The formative time lag on the other hand is much faster than the statistical time lag and more importantly it is relatively constant. The formative time lag is the time taken for the avalanche to cross the gap. The formative time lag is dependant on the percentage overvoltage under impulse conditions. In other words, as the ratio $\frac{V_a - V_b}{V_b}$ increases. Where V_a is the applied voltage and V_b is the breakdown voltage of the gap. On average it is in the region of $0.01\mu s$

The above mentioned parameters (ionisation mechanisms, attachment coefficient and breakdown under pressurised conditions) and their affect on the phenomenon of laser-triggered breakdown will be further discussed in chapters 3 and 7.

2.8 Conclusion

There are three main mechanisms that are used to describe electrical breakdown in gases. These are the Townsend, Streamer and Leader mechanism. The leader mechanism is used to describe breakdown across long gaps (over a meter). The streamer process s able to explain breakdown across gaps where the electric field is not uniform. For example a plane to point gap.

There are many ways by which electrical breakdown can occur. The most important of these process is ionisation by electron collision. At the same time processes such as photoionisation, ionisation by metastable atoms and to a lesser degree thermal ionisation become important.

In some cases gases such as the halogens are able to attach free electrons and form negative ions. These gases are known as electronegative and the process of electron attachment counteracts that of ionisation. Therefore, the breakdown of a gap depends on the combination of ionisation and attachment.

The phenomenon of electrical breakdown is dependent on the pressure of the

gas and the electric field applied to the gap. The law that describes the relationship between the breakdown voltage and the gap pressure and electric field, is known as Paschen's Law ($V = f(pd)$).

There are two types of time lag that are associated with gap breakdown. These are the statistical and formative time lag. The statistical time lag is the time taken for an electron to become available and start the breakdown process, whereas the formative time lag is the time taken for the electron avalanche to cross the gap. The first, as the name implies is highly variable, whereas the formative time lag remains relatively constant.

Chapter 3

Laser Background

3.1 Lasers and laser parameters

3.1.1 Lasers in general

The term laser is an acronym for Light Amplification by the Stimulated Emission of Radiation. This term was first used in 1960 when the first laser was built [8]. Laser light differs from normal light because of its following three main properties:

- Laser light is *Monochromatic*. This means that all the photons that comprise the laser beam are of the same wavelength. This is not the case with visible light for example. Visible (white) light is made up of all seven visible colours (from violet (400 nm) to red (700 nm)) [9].
- Another property of laser light is that it is *directional*. In other words, the divergence of the beam is very small. A laser beam, unlike normal light, does not diverge (does not expand) quickly. This means that the beam size remains fairly unchanged over long distances.
- Finally, laser light is *coherent*. The photons that are generated by the laser are all in phase with each other. The combination of these features make laser light very important. Lasers are used in many aspects of life. Lasers are used in devices such as CD players, they are used in the medical world (for surgery) in industry for welding and cutting

and in scientific research for performing spectroscopy and in the field of nanotechnology [10]. Lasers are also used extensively in the military for various purposes such as range finding and targeting.

3.1.2 Laser Operation

The basis of laser operation is what is called stimulated emission of photons. When an electron is given energy, it rises to a higher energy level. When that electron returns to its original state, the energy that was absorbed is now released in the form of a photon. This is how light is emitted. In most cases, this process happens spontaneously and without any external stimulus.

With stimulated emission, the mechanism is slightly different. In this case, a photon, whose frequency matches the gap between the higher and lower energy states, is directed into a system of molecules, some of which are in the exited state. Each molecule can now return to its original state. The result is the emission of a photon. The emitted photon has now the same frequency as the supplied radiation. The most important part of a laser is the active medium used. This will be the source of the photons that will comprise the laser beam. In other words, this the medium in which stimulated emission will occur. The active medium can be of very different substances. These can either be gases, liquids or solids. For example, the first laser that was built used a ruby rod as its active medium. The most common gases that are used are helium, argon and carbon dioxide. A laser is made up of three fundamental parts: The active medium, a fully and a partially reflective mirror. The arrangement can be seen below in *figure 3.1*

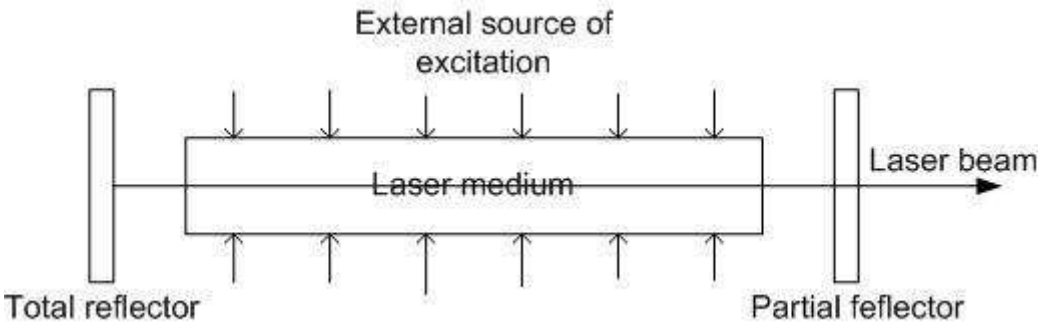


Figure 3.1: Operation of a laser

In reality, the back reflector reflects only about 99% of the incident photons. The partial reflector is a 60% mirror. Various types of lenses can be used depending on the application.

The type of excitation also varies. Two of the most common excitation mechanisms are optical and electrical. Optical excitation is used with solid state lasers such as the Yttrium-Aluminium Garnet (YAG) lasers. In this case, a high intensity flash lamp is used to provide the necessary excitation. In the case of gas lases such as the KrF excimer or the nitrogen laser, electrical excitation is used. In other words, an electrical discharge is used to stimulate the active medium.

Lasers are also divided into two distinct groups depending on the type of beam emitted. Therefore we have Continuous Wave lasers and pulsed lasers. In this document, the emphasis is placed on Pulsed Lasers.

3.1.3 Laser Parameters

The most important aspect of a laser is the outputted beam. The laser beam has many parameters associated with it. Such parameters include wavelength, physical size (and mode), energy density (fluence) and power density (intensity). These parameters are important when for example choosing the correct laser for a certain application.

Fluence

A laser beam has an energy density. This quantity is known as fluence and is measured in J/cm^2. The general expression for fluence (in the case of a gaussian beam) is $\phi(x,y) = \phi_0 e^{-2[\frac{x^2}{\omega_x^2}+\frac{y^2}{\omega_y^2}]}$ where ϕ_0 is the peak fluence and ω_x and ω_y are the beam waists in the x and y direction respectively. This energy can be easily measured by a suitable energy detector.

Intensity

In the same way that fluence is defined as energy density, intensity is defined as power density. The intensity of a laser beam is expressed in W/cm^2 . In pulsed lasers, the average power output of the laser is given by the ratio of total energy to pulse width i.e. $P = \frac{E_{total}}{\tau}$ where τ is the pulse width. The shorter the pulse, the higher the output power of the laser. The Intensity of the beam is given by the ratio of power to area i.e. $I = \frac{P}{A}$. This means that by reducing the area, the intensity of the beam increases. This can be achieved by focusing the beam with suitable lenses.

Wavelength

The wavelength output of the laser is dependent on the active medium used. Each active medium is able under stimulated emission, to produce photons of a certain wavelength. For example, the fundamental wavelength of an YAG laser is 1064 nm (near infrared). A simple He laser emits red light at 632 mn. An KrF excimer laser can produce a UV laser beam at 248 nm (UV-C). In the case of the YAG laser, with certain types of crystals, the wavelength can be shifted through the other harmonics which include 532, 355 and 266 nm. The drawback is that by reducing the wavelength, the output energy decreases.

Beam type (shape)

The beam shape is one of the most important properties of a laser. If the beam quality is good, then all the other parameters (except wavelength which depends on the active medium) improve in efficiency. Since the laser beam is created by setting up standing waves in the laser cavity, it can be said that the beam can have different modes. These are known as TEM (transverse electromagnetic) modes.

The simplest TEM mode is TEM_{00} This occurs when wave propagation happens parallel to the axis of the laser. If the wave propagation is slightly offset,

the laser beam will have modes other than TEM_{00}. This represents a multinode beam and is depicted by TEM_{pq} . Increasing the number of modes in the beam does increase the intensity of the beam, but in practice, it is more advantageous to keep the beam as gaussian as possible. In fig. 3.2, one can see three different TEM modes.

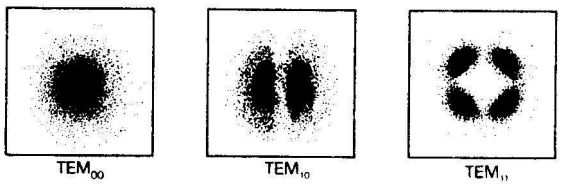


Figure 3.2: Some common modes for lasers

3.2 Laser-induced breakdown

The phenomenon of laser-induced breakdown was first observed in 1963 by Marker, Terhume and Savage. It was found that a laser pulse from a Q-switched ruby laser was able, after focusing, to create a spark in air. This spark was similar to that produced in a spark gap situation. Since then, research has been performed in order to understand the physical mechanisms that govern this phenomenon.

Through research it has been found that when a laser beam of intensity in the order of about 100 GW/cm^2 [11] interacts with a gas, a spark is developed at the focal point of the lens used. The intensity of the beam required varies from gas to gas and depends on various parameters such as the gas used, the wavelength and energy of the beam and the lens used.

There are two main mechanisms by which laser-induced breakdown occurs. These are the electron cascade and multiphoton process. The latter is the most important of the two processes. In multiphoton ionisation, a gas molecule (or atom) may absorb more than one photon simultaneously. The probability of this type of ionisation occuring is highly dependent on the number

of photons per unit area. In other words, it is dependent on the photon flux. In fact the probability is proportional to the n_{th} power of the photon flux i.e. $p \propto \Phi_{photon}^{n}$ [12]. For example, the ionisation potential for oxygen (O_2) is about 12 eV (12.071). Therefore, for a laser operating at 1064 nm (1 eV per photon), about 12 photons will be required to ionise an oxygen molecule [13].

As mentioned, one the most important parameters that govern the process of laser-induced breakdown is the laser beam intensity. The laser beam intensity is primarily dependant on the time pulse of the laser, on the quality of the focusing and on the type of lens used (in terms of focal length). The shorter the time pulse of the laser, the higher the power output. On the other hand, the shorter the focal length of the lens used, the higher the fluence and consequently the higher the energy density. There is though a drawback: The shorter the focal length used, the shorter the spark generated. If a longer lens is used, then the spark generated tends to be much longer [14]. This may be a problem when a laser beam is used to break down a spark gap. It may be more advantageous to generate a longer spark.

The average intensity required to generate a spark in a gas is about 100 GW/cm^2. It may vary though from gas to gas (depends on the type of gas and its atmosphere i.e. temperature and pressure). It also depends on the laser wavelength. For an Nd:YAG laser with a pulse width of about 8 - 10 ns, and a 100 mm lens, laser induced breakdown of air occurs at about 70 mJ /pulse (one laser shot and 100% probability of breakdown on that shot). Some gases are able to absorb the energy of some wavelengths better then others.

3.2.1 Calculation of laser beam intensity

The laser beam intensity or power density is determined by three parameters: The pulse width of the laser, the spot size i.e. the size of the beam after focusing and the energy contained in the pulse. The pulse width of a laser is defined as the Full Width Half Maximum pulse width (FWHM) (*figure 3.3*).From this, it can be seen that the intensity I can be expressed mathematically as follows:

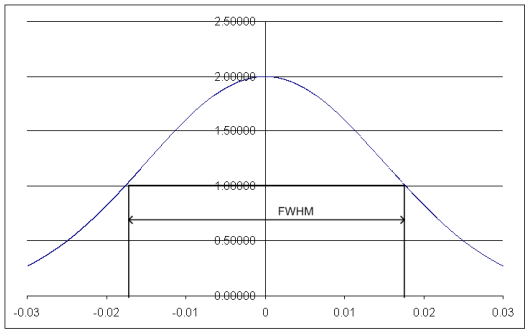


Figure 3.3: Definition of a FWHM pulse

$$I(x, y, t) = I_0 g(t) f(x, y) \tag{3.1}$$

Where I_0 is the peak intensity of the beam. From this relationship, it can be seen that intensity is dependant on the time pulse and the beam shape. It is also known that the energy is the integral of the intensity:

$$E = I_0 \int_0^\infty \int_A I(x, y, t) dA dt \tag{3.2}$$

The energy E can be measured by means of an energy meter. The pulse width can also be measured with a fast detector such as a photodiode. From these values one can calculate the peak intensity I_0. The intensity plot is then obtained by plotting equation 3.1 and taking $t = t_0$ i.e. when $g(t_0) = max[g(t)]$

For example consider the simple case of a lease beam that has the following parameters:

- beam size: 0.25 by 0.13 cm
- pulse width: 25 ns Full Width Half Maximum (FWHM)
- energy: 230 mJ/pulse

The beam size and pulse width can be approximated as square pulses of width 0 to 0.25 cm (x-direction), 0 to 0.13 cm (y-direction) and 0 to 24 ns respectively.

For this situation, the peak power can be calculated as follows:

$$I_0 = \frac{E}{\int_0^{\tau}\int_0^{x}\int_0^{y} g(t)f(x,y)dxdydt} \Rightarrow I_0 = \frac{230mJ}{\int_0^{25ns}\int_0^{0.25}\int_0^{0.13} 1\cdot 1\cdot 1 dxdydt}$$

From the above, the following is obtained:

$$I_0 = \frac{230mJ}{25ns\times 0.25cm\times 0.13cm} = 283MW/cm^2$$

The function therefore that describes the intensity plot is as follows:

$$I(x,y,t_0) = I_0 g(t_0) f(x,y) \overset{g(t_0)=1}{\rightarrow} I(x,y,t_0) = 283 f(x,y) MW/cm^2$$

As mentioned, this example does not take into account a complicated beam shape or a real time pulse waveshape. In this case, one would have to perform numerical integration in order to obtain the correct intensity plot.

3.3 Laser-triggered spark gaps

In the previous section, a brief overview of laser-induced breakdown in gases. In this section, information on laser-induced electrical breakdown of spark gaps will be presented. As mentioned, a high intensity laser beam is able to create a spark in air. This means that if this spark were to be generated in the region of a high electric field (e.g. in the region of a spark gap), electrical breakdown of the gap would occur. This concept has many applications especially in high speed and accurate high voltage switching.

In high voltage engineering, spark gaps are often used as switches. In many instances, spark gaps are designed in such a way that they can be externally triggered. Most of the triggered spark gaps used are mechanical in nature. Even though these type of gaps are very simple to manufacture and operate, the switching times are sometimes too slow.

There are three main types of triggered spark gaps. The first and most common of the three, is a three electrode gap known as the trigatron. The other two

are the field distortion gap (also a three electrode gap) and the laser triggered spark gap. In the case of the trigatron, a high voltage pulse is used to initiate a spark on the main sphere. In many cases, a spark plug is employed to generate the spark. The presence of this spark across the annular gap (it is normally set to 1 mm) of the trigatron, then causes the main gap to breakdown. A simple drawing of a trigatron can be seen in *figure 3.4*

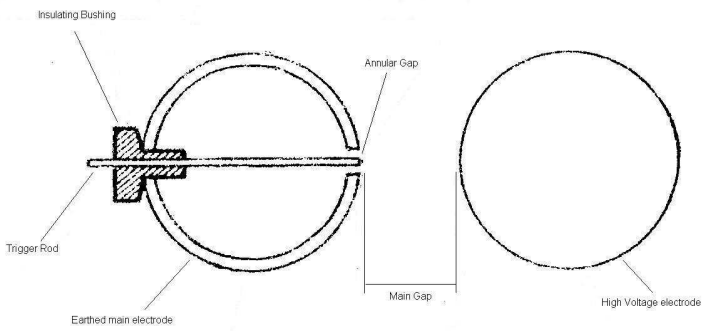


Figure 3.4: Operation of the trigatron

The other three electrode triggered spark gap is the field distortion gap. It works on a principle similar to the trigatron. A simple diagram can be seen in figure 3.5

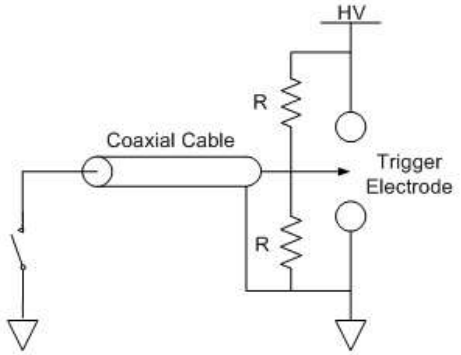


Figure 3.5: The field distortion gap

The principle of operation is as follows: A high voltage is set up across the two main electrodes. A third electrode is then placed in the middle of the main gap. This auxiliary electrode is biased to exactly half the voltage across the

gap. In order to trigger the breakdown process, a high voltage pulse is applied to the trigger electrode. This pulse causes a momentary distortion of the electric field in the region of the spark gap. The result is electrical breakdown.

The third type of spark gap that will be discussed, is the laser triggered spark gap. In this case, a high intensity laser beam is used to cause ionisation in the region of the gap. In essence, the laser beam is used to provide the seed electrons needed to start the breakdown process and thus eliminating the statistical time lag.

There are many ways to design and build such a triggering mechanism. There are two main geometries for laser-triggered spark gaps. The laser beam can be either perpendicular to the axis of the gap, or shone in the direction of this axis as can be seen in figures 3.6 and 4.10

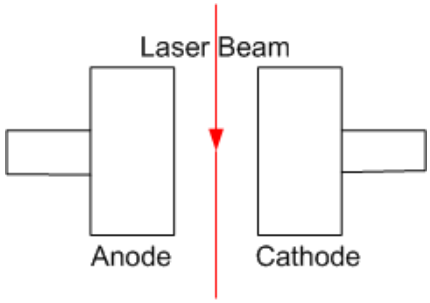


Figure 3.6: Perpendicular spark gap arrangement

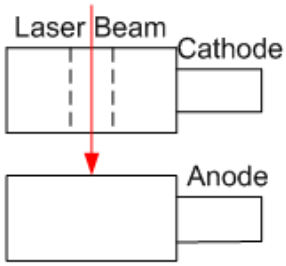


Figure 3.7: Coaxial spark gap arrangement

In the case of the perpendicular spark gap arrangement, the laser beam is focused perpendicular to the axis of the gap. This mechanism operates on

air ionisation alone. The focused laser beam is able to deliver enough power density to cause ionisation of air (generation of a spark in air) thus leading to the desired electrical breakdown. The advantage of this set up is that since the laser beam does not interact with the electrodes, no ablation occurs [15]. The result is that electrodes will generally last longer. The disadvantage is that the voltage range obtained is large and it depends on where the laser beam is focused in the gap. The voltage range becomes smaller as the focus approaches the cathode [16]

On the other hand, in the case of the coaxial geometry, there are several mechanisms in play: In the one instant, the laser beam is able to ionise air (as in the case of the perpendicular arrangement). At the same time, electrode ablation occurs. The laser beam is able to ablate the surface of the electrode (anode or cathode). The result is that electrode particles are released into the high electric field of the gap assisting in the breakdown process. In the coaxial geometry, another advantage is that the laser beam may help create an ionisation channel along the axis. The voltage ranges obtained in this case are much smaller than in the perpendicular arrangement

The range of the laser-induced breakdown voltage is also dependent on factors such as the gap size and the gap atmosphere. The longer the gap, the higher the maximum voltage that the gap will be able to withstand. At the same time, the minimum voltage that the laser will be able to break down, will also increase. This is because the laser beam will not be able to create enough ionisation in the gap. The gap size chosen is dependant on the desired range. In the experiments a 5 mm gap was chosen.

Another way to alter the range would be by altering the gap atmosphere. In other words, changing parameters such as the gas type and the pressure or temperature of the gas. The key parameters that one must take into account when choosing a gas for laser-triggering applications is the ionisation potential, its electronegativity and its absorption spectrum. Inert gases such as Xenon or Helium can be used since they have a low ionisation potential and a relatively large cross-section area [17]. Another approach would be to use a highly

electronegative gas such as SF_6 [18, 19].

Sulphur hexafluride is very strong electronegarive gas. Its breakdown strength at atmospheric pressure is approximately 89 kV/cm. This is nearly 3 times higher than the breakdown strength of air [2]. The advantage of using SF_6 in a switching application, is that once the integral of $\int (\alpha - \eta)$ exceeds the value of 18, the gas breaks down. This can be achieved by the application of a very high intensity electric field. This field can be provided by a high intensity laser beam. The overall advantage of using SF_6 is that one could obtain a very large breakdown voltage range.

By considering the absorption for SF_6, it can be seen that there is a large peak at 10000 nm (see *figure 3.8*). Therefore, one could use a hig power CO_2 laser to obtain better results. A CO_2 emits light in the far infrared region and has a wavelength of 10 microns.

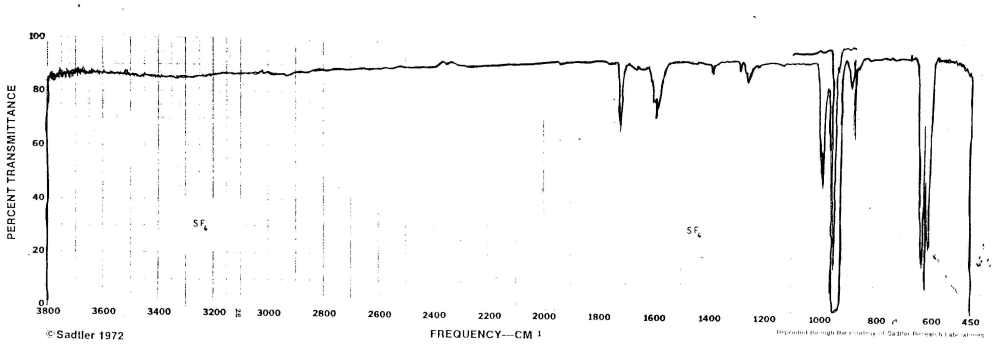


Fig. 2. Infrared spectrum of sulfur hexafluoride; 10-cm path length cell, with KBr optics; cell pressure: curve A (complete scan) 2.666 kPa (20 mm Hg), curve B (partial scan) 0.0667 kPa (0.5 mm Hg) (5).

Figure 3.8: Absorption spectrum of SF_6

In this research project though, the focus is on using laser light in the UVB band (248 nm) produced from an KrF Excimer laser.

3.4 Conclusion

In this chapter a background into the operation of lasers was presented. At the same time, information on the various parameters that govern the design of a laser-triggered spark gap was discussed. Laser-induced electrical breakdown depends heavily on parameters such as laser beam intensity (proportional to spot size), laser wavelength and spark gap geometry and atmosphere. For the experiments to be done for this project, a 5 mm gap was used at atmospheric pressure and room temperature. The electrodes were placed in a coaxial geometry and they were made of brass. In the following chapter, the design and construction of the impulse generator used will be presented. The impulse generator was used as the source that will set up the voltage across the laser-triggered spark gap.

Chapter 4

The impulse generator

4.1 Introduction

Impulse generators are generally used to create lightning waveforms in a laboratory environment. From research done on lightning, various standard waveform have been developed in order to simulate the effects of a direct or an induced lightning strike on various devices under test. Such devices may include surge arrestors, switchgear, electronic devices etc. In this research project, a simple impulse generator was designed in order to provide a high voltage (magnitude of current not important) across the electrodes that comprise the laser triggered spark gap. The voltage range the generator would be able to attain is 0 to 20 kV. This section includes the theory of operation and design for such a generator. It will also include a description of the design and construction process for the impulse generator in question.

4.2 Impulse waveforms

One of the most important source of overvoltages on power systems originates from direct or induced lightning activity. During a direct lightning strike, the peak current that is injected in to the struck object can be in the order of 100 kA. Adjacent lightning strikes can also induce very high voltage transients in various electronic equipment. In lightning strikes, the produced transients are very fast and depend on the rate of change of the lightning current. This

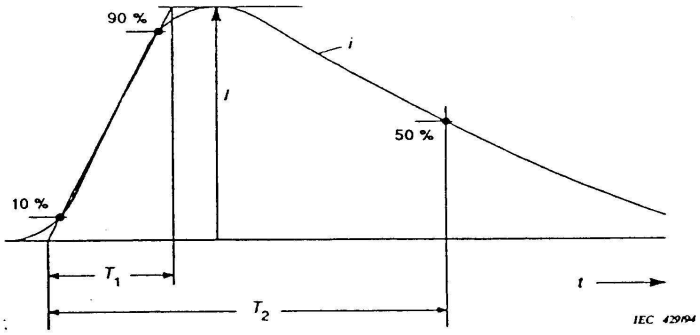


Figure 4.1: Impulse waveform definition

rise can be of the order of 100 kA/μs [20, 21].

Switching phenomena are another cause of surges. In this case though, the transients are much slower than in those of lightning strikes. The amplitudes of these waveforms are related to the operating voltage and the waveshape is dependent on the switching conditions. It is known though that the shape of these surges can be very dangerous under certain conditions (such as atmospheric air insulated systems).

For these reasons, a set of standard waveforms have been developed that can be used to reproduce the effects of lightning and switching surges. The general shape of these waveforms is expressed in the IEC 60-1 document [22] and can be seen in *figure 4.1.*

According to the standards, an impulse waveform is characterised by its peak value and the rise and fall time. The rise time T_1 is defined as the time taken for the current (or voltage) to reach 90% of its peak. More precisely, it is the time taken from 10% to 90% of the peak value. The fall time T_2 is defined as the time taken for the current (or voltage) to drop to 50% of the peak value. Therefore, if the peak value is I_{max}, the rise time is T_1 and the fall time is T_2, then an impulse is defined as I_{max}, T_{rise}/T_{fall}.

4.2.1 Lightning impulse

In the case of a lightning impulse, there are two distinct waveforms that are of importance. These are the 1.2/50 voltage waveform and the 8/20 current waveform. The lightning waveforms are defined in the SABS IEC 61024-1-1:1993 standard [23]

The lightning current is defined as follows:

- Rise time (10% to 90%): 8 μs $\pm$ 1 μs
- Fall time (drop to 50%): 20μs $\pm$ 2 μs

The voltage waveform is defined as

- Rise time (10% to 90%): 1 μs $\pm$ 30 %
- Fall time (drop to 50%): 50μs $\pm$ 20 %

4.2.2 Switching surge

A switching surge as mentioned, is very much slower than an lightning impulse. The parameters of such a surge are as follows:

- Rise time (10% to 90%): 250 μs $\pm$ 20 %
- Fall time (drop to 50%): 2500 μs $\pm$ 60 %

4.3 Impulse generators

In order to generate lightning impulse and switching surge waveforms, a suitable impulse generator is required. Impulse generators can be divided into two main categories: Current and voltage impulse generators. As the name implies,

a current impulse generator is used to produce high energy current impulses, whereas a voltage impulse generator is used to generate voltage waveforms. A typical impulse generator circuit can be seen in *figure 4.2*

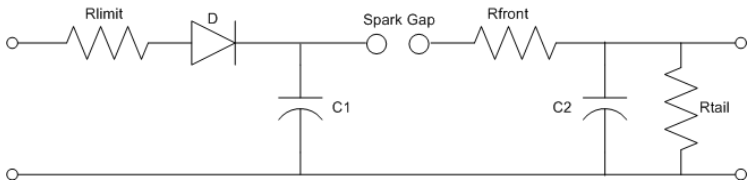


Figure 4.2: Impulse generator circuit

In the circuit in *figure 4.2*, one can identify 3 main sections. These are the rectifying circuit, storage capacitor and waveshaping circuit. The rectifying circuit is made up of a current limiting resistor and a rectifying diode. The main aim is to convert the High voltage AC input (generated by a HV transformer) into a DC voltage. The quality of the DC output is not of great significance. As long as it is able to charge the storage capacitor. The current limiting resistor is used in order to protect the diode and to ensure that it operates effectively.

The storage capacitor (C_1 in the circuit) is the next important component of the circuit. This capacitor will be the one that stores the charge that will be converted to a impulse waveform. Depending on the desired amplitude of the output waveform, a single capacitor or a capacitor bank may be used. In the case of a multistage impulse (Marx) generator, a set of capacitors are used in cascade as can be seen in *figure 4.3* (for a four stage generator).

Finally, the waveshaping circuit, as the name implies, sets the rise and fall time of the impulse. It is made up of three components: two resistors and a capacitor. These are R_{front}, R_{tail} and C_2 in *figure 4.2*. It can be shown that for an impulse generator, the rise and fall time can be given by the following formulas:

$$T_{rise} = 3.25 R_1 C_2 \tag{4.1}$$

$$T_{fall} = 0.69 R_2 (C_1 + C_2) \tag{4.2}$$

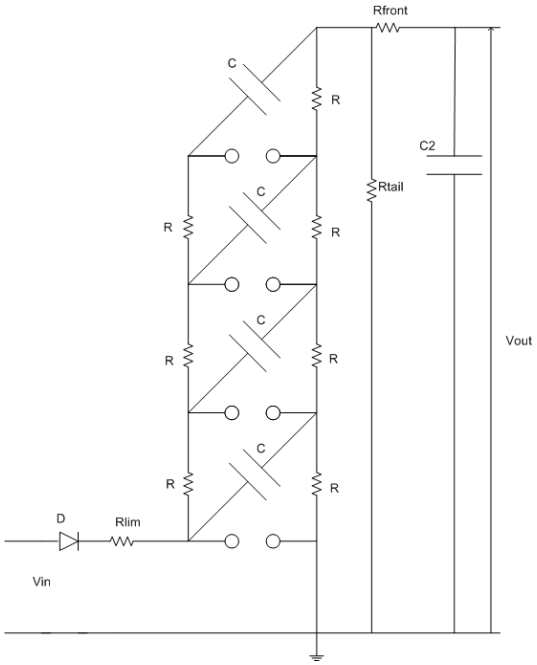


Figure 4.3: Marx impulse generator circuit

4.3.1 Impulse generator efficiency

The impulse generator efficiency is defined as the ratio of the output voltage to the charging voltage. This ratio can be expressed as a percentage according to the relationship:

$$\%\eta = \frac{V_{out}}{V_{charge}} \times 100 \tag{4.3}$$

The efficiency is set by the waveshaping circuitry. This is because is depends on how fast the storage capacitor and the regulating capacitor at the output are drained. The faster C_1 and the slower C_2 is drained, and the higher the efficiency of the generator.

4.4 Impulse generator design process

4.4.1 Requirements

In this project, the main aim was to supply a voltage of about 20 kV to a laser-triggered spark gap. It is also important to note that the shape of the output waveform is not of great importance. The generator was not required to generate waveforms with high energy content. In other words, the generator was not to be used to produce high currents. A high voltage output is all that was required. The generator was also required to be as compact as possible and light enough to transport.

4.4.2 Simulations

The generator model

In order to design the impulse generator, a Matlab Simulink model was used. This model can be seen in *figure 4.4*.

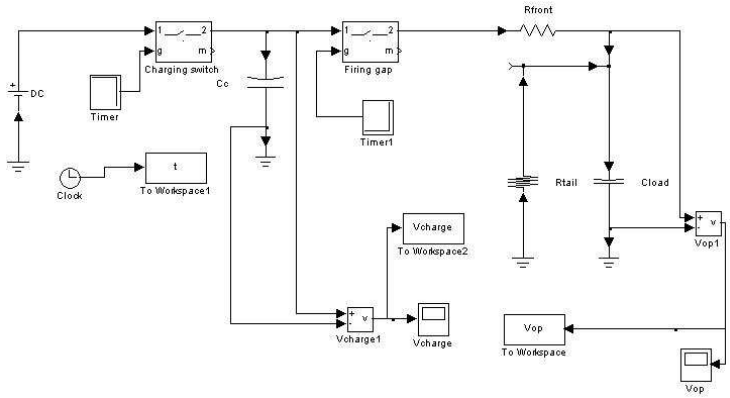


Figure 4.4: Simulink impulse generator model

In essence, this model is a reflection of the impulse generator circuit shown in *figure 4.2*. In this model, the rectifying circuit (current limiting resistor and diode) have been replaced with a DC voltage source. The user can therefore enter various values of charging voltage and monitor the output. The voltage source is connected to the impulse generator circuit via a time-controlled

switch. The switch was set up in such a way, that at time zero, the switch will be closed. After 1 ms, the switch changes state and opens. This means that the charging capacitor C_c will be charged for 1 ms.

The other key concept is the modelling of the spark gap. The spark gap was also modelled as a time controlled switch. The gap is initially open. After a time of 2 ms (that it one ms after the completion of the charging process), the timer forces the switch to charge state and close. This enables C_c to discharge completely through the spark gap and into the waveshaping circuitry. In this model, all capacitors were allocated zero inductance and resistance, whereas all resistors were given no inductance and infinite capacitance.

In order to obtain results from the simulations, the following was done. The voltage between the charging capacitor and the output (across C_{load} were measured by means of the voltmeter block and the voltage was plotted on an oscilloscope screen. In order to process the results and calculate parameters such as the percentage efficiency of the model, two varibles were generated (Vop and Vcharge). These were imported into a simple m-file for processing. This m-file can be seen in *Appendix A*.

Results obtained from simulations

The simulations, as mentioned, were performed for various values of capacitance and resistance and also across a voltage range from 1 kV to 20 kV. The components for the generator were selected through a combination of simulation results and availability. The best results in terms of efficiency, were obtained for the following values of capacitance and resistance:

- C_c=12.5 nF
- C_{load}=2.5 nF
- R_{front}=374 Ω
- R_{tail}=119.6 kΩ

With these values for the passive components of the circuit, the efficiency of the generator remained relatively constant at 83%. (82.8 - 82.9%). Below, one can see the results of the simulation for a voltage of 2 kV.

Charging Voltage: 2 kV
Output Voltage: 1.658 kV
Percentage Efficiency: 28.9%

The impulse waveform can be seen in *figure 4.5*

From the graph of the impulse, one can evaluate its rise and fall time. A matlab m-file was written in order to compute the rise and fall time of the impulse. This m-file can be seen in *Appendix A*

After processing the data, it was found that the waveform has a rise time of about 1.7 μs and a fall time of 1200 μs. As mentioned, the shape of the impulse is of no great importance. This means that the generator is able to perform at the highest possible efficiency.

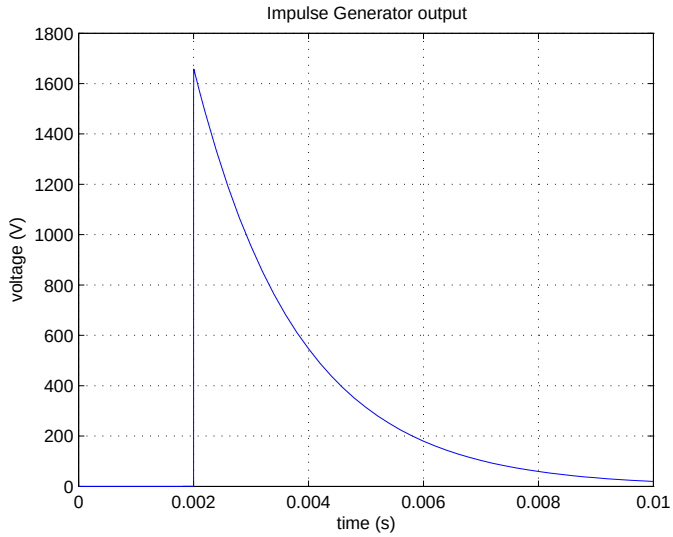


Figure 4.5: Impulse waveform for a 2 kV charging voltage

4.5 Building and testing the generator

In order to conduct the experiments dealing with laser triggering of spark gaps, a suitable high voltage source had to be provided. For this reason a simple voltage impulse generator was designed and constructed at the GEN-MIN laboratories of the School of Electrical and Information Engineering at the University of the Witwatersrand.

The requirements of the generator in terms of operation can be seen below:

- Low energy output (i.e. low current)
- Output voltage up to 20 kV
- Waveshape that will ensure a high enough efficiency (over 80%)
- Generator equipt with a suitable spark gap that will allow for laser triggering

The generator was designed as a single stage impulse generator according to the circuit diagram of *figure 4.2*. During the building of the generator, steps

were taken (where possible) to minimise the effects of inductance on the system.

The electrical components that were used can be seen below:

- 12.5 nF ceramic capacitor rated at 30 kV
- 2.5 nF ceramic capacitor rated at 30 kV
- 80 kV rectifier diode (SKXA75M)
- 380 kΩ resistor
- 348 Ω resistor
- 119 kΩ resistor

The entire circuit was mounted on a small wooden table. The 80 kV diode and the 380 kΩ current limiting resistor were mounted on the same bracket. A simple drawing of this arrangement can be seen below:

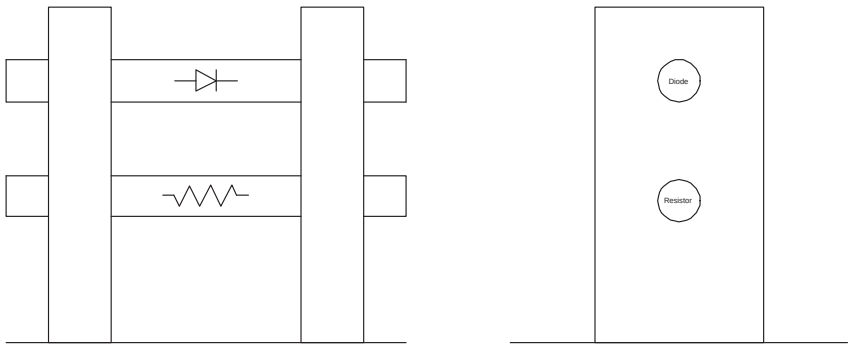


Figure 4.6: Front and side view of the bracket used to mount the diode and current limiting resistor

A picture of the bracket that was built can be seen in *figure 4.7*

4.5.1 Electrical components and connections

The high voltage AC input was supplied by means of a 30 kV transformer (low current). An autotransformer (variac 230/230 V) was used to vary the

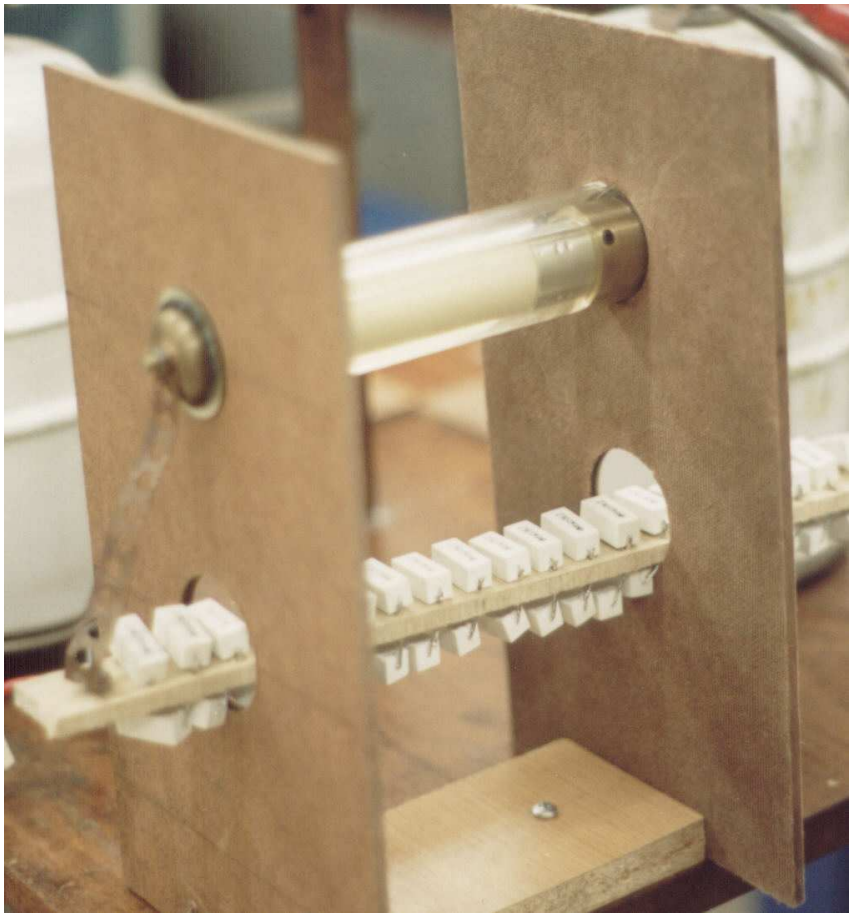


Figure 4.7: The charging circuit of the impulse generator

output of the transformer from 0 to 20 kV. The current limiting resistor was made up from about 50 carbon resistors connected in series. As mentioned, a diode (Semikron SKXA75M) was connected in series with the resistor in order to provide a suitable DC input to the generator. This arrangement provides half-wave rectification which in this case is sufficient to charge capacitor C_1.

Both capacitors (charging and waveshpaing) were bolted onto the wooden table. Ground connections were provided by means of 60 mm wide and 1 mm think copper strips. Copper strips were also used to connect the various electrical components together. All connections were made a short as possible in order to minimise the effects of inductance. A simple bushing made from perspex was used to provide insulation for the high voltage output terminal of the gerenator. A simple drawing of this bushing can be seen below:

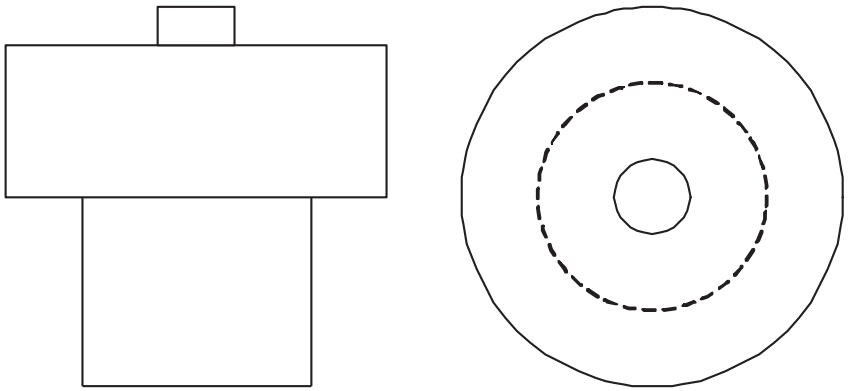


Figure 4.8: Front and side view of the insulating bushing

A picture of the bushing mounted on the impulse generator can be seen in *figure 4.9*



Figure 4.9: Bushing mounted on impulse generator

4.5.2 The spark gap

as mentioned, the impulse generator in question would be used for laser triggering experiments. The principle of operation is that a laser beam will be used to cause ionisation in the area of the spark gap and thus lead to electrical

breakdown. The electrodes were placed in a coaxial arrangement. as seen in *figure 4.10*

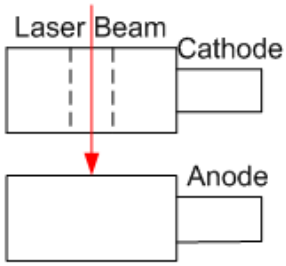


Figure 4.10: Coaxial spark gap arrangement

This setup has its advantages and disadvantages. It has been found that a coaxial spark gap geometry is far more effective [16]. This is because at the same time electrode particles are released into the space of the gap due to laser beam ablation. These particles assist in the breakdown process. For the perpendicular arrangement to be effective, the laser beam must be fired close to the cathode.

The gap was designed in such a way that the actual spark gap distance can be varied by up to 40 mm. The electrodes were made from brass and were cylindrical in shape. The electrode arrangement was the same as in fig. 4.10. Each electrode was 10 mm in hight and 15 mm in diameter. A 5 mm hole was made in the cathode in order to allow the laser beam to enter the spark gap. The pressure in the gap was set to atmospheric (the gap was open to air). At a later stage, a new spark was made to contain SF_6 under pressure. This gap will be discussed at a later stage.

4.5.3 Experimental performance

Once the generator was built, it was tested for its efficiency. The generator was triggered by increasing the voltage up to the point where the air in the gap broke down. By adjusting the gap size, various voltage levels could be obtained (taking into account a rough rule of 30 kV/cm for dry air). The

waveforms were recorded by means of digital oscilloscope (waveforms saved on floppy disk). A table of the charging and output voltage obtained can be seen in *table 4.1*

Charging Voltage	Output Voltgae	% Efficiency
0.9	0.736	81.8
2.3	1.88	81.7
3	2.44	81.3
4.1	3.36	82.0
5.5	4.56	82.9
6	4.76	79.3

Table 4.1: Experimental results obtained from the impulse generator

From this table, it can be seen that the % Efficiency of the generator is about 82%. This corresponds with the theoretically obtained results for the generator performance (Simulink model). This means that the generator is able to produce enough voltage to perform the laser triggered spark gap experiments successfully. From simulations it was seen that the output voltage was a 1,7/1200 microsecond waveform. Experimental results showed that the fall time was much shorter than 1200 μs. It was found to be about 350 μs (the fall time). The rise time was also measured to be slightly faster about 0.5 μs. In *figure 9.21*

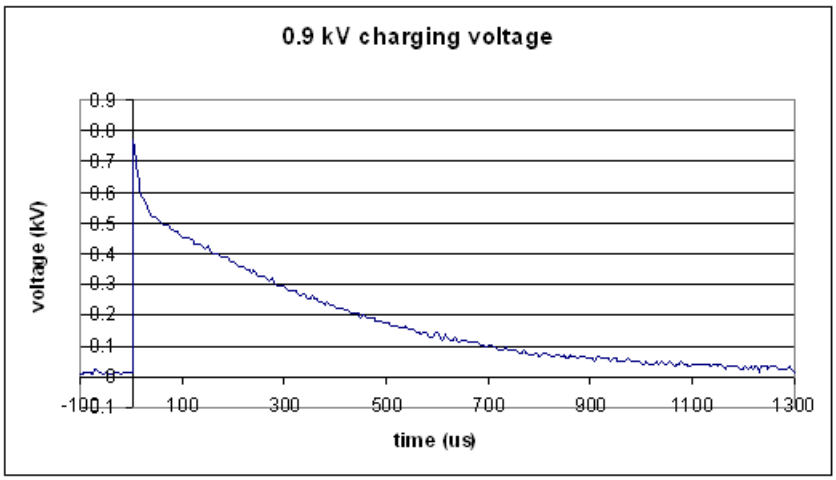


Figure 4.11: Output waveform for a 900 V charging voltage

One problem though that was noted, was the fact that at higher voltages (over 6 kV), a lot of restriking took place. This can be attributed to the following: In

some cases, when electrical breakdown takes place, there is too little energy in order to sustain the arc across the gap. In other words, the breakdown process starts and then at some point stops. The process is then can restart and the arc crosses the gap. This can be seen in *figure 4.12*. Here at about 400 μs after the breakdown has started the process stops. at 400 μs, a restrike occurs and the process this time continues and successfully discharges the charging capacitor. It is interesting to note that when the laser was used, this phenomenon of restriking was eliminated.

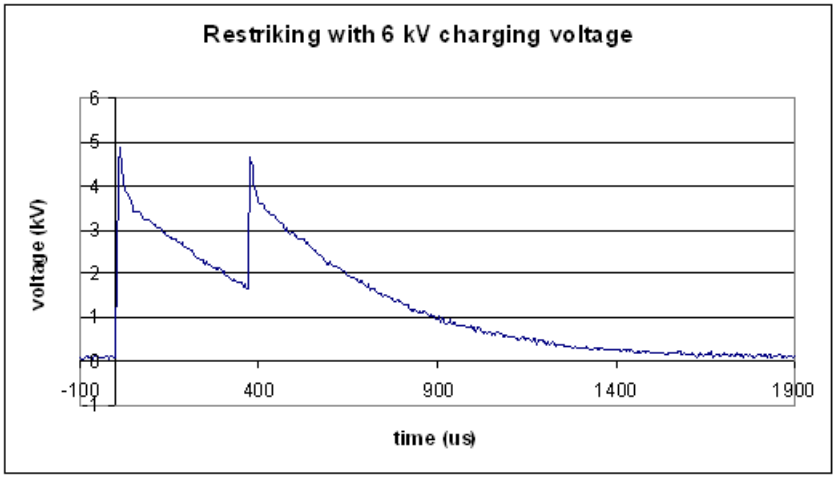


Figure 4.12: Output waveform for a 900 V charging voltage

4.6 Conclusion

In this chapter, an overview of the design, building and testing of a simple single stage impulse generator was presented. The impulse generator that was designed was able to produce output voltages up to 20 kV. The efficiency of the generator (defined as the ratio of the output vs. the input voltage) was found to be about 82%. This correlelates well with the results obtained from simulations. A simple spark gap was designed to allow the gap to be triggered by means of a laser beam. The electrodes of the gap were arranged in a coaxial geometry. In the following chapters the experimental results will be presented for work done on the two lasers used in this project. These are namely a KrF eximer operating at 248 nm and a Nd:YAG operating at 1064, 532 and 355 nm.

Chapter 5

Experiments with the KrF Excimer laser

5.1 Introduction

In the previous chapters, a literature survey of the background work to this project was presented. This included background in electrical and laser-induced breakdown, laser operation and impulse generator design. In the following chapters, the experimental work done on two lasers will be presented. In particular, a KrF excimer operating at 248 nm (230 mJ pulse energy and 25 ns pulse width) and a Nd:YAG operating at 1064, 532 and 355 nm (170 mJ max pulse energy, 8-10 ns pulse width) were used. The impulse generator discussed in chapter 4 was used to provide the voltage across the laser triggered spark gap.

5.2 The KrF laser and equipment set up

The excimer laser used in this project is located at the National Laser Centre at the CSIR in Pretoria. A picture of the general set up of the lab can be seen in figure 5.1

In this figure, one can see in the background the KrF laser (LPX 200). In the

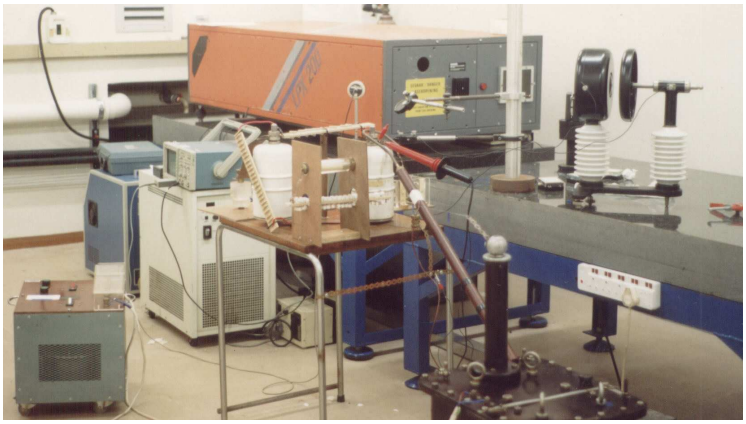


Figure 5.1: KrF laser set up at the CSIR

foreground, one can see the impulse generator, the high voltage transformer and the variac used to supply the voltage for the laser triggered spark gap.

The first step was to measure the beam parameters. These include beam size, energy and pulse width. The beam size was measured by means of burn marks on heat sensitive paper (standard fax paper) as can be seen in figure 5.2

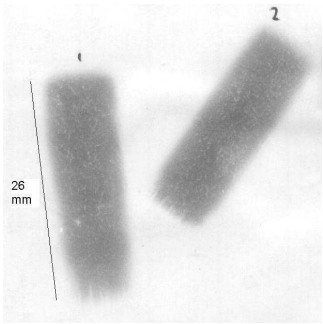


Figure 5.2: Beam shape of the KrF laser

From this image, one can see that that the beam coming out of the laser is rectangular with dimensions of 26 mm by 8 mm. This makes the beam difficult to focus with normal lenses.

The energy of the laser was measured by means of an energy detector. The detector used can be seen in figure 5.3

The laser energy output was found to be about 230 mJ per pulse. The laser



Figure 5.3: Energy meter used

was operating at a repetition rate of 1 Hz (essentially in single shot mode). the reason for this was that a successful breakdown event was defined as the ability of the beam to break down the gap after one laser shot.

As far as the pulse width was concerned, a fast detector such as a photodiode was used. The beam was allowed to scatter of a non-reflective surface such as cardboard or polystyrene. The detector is then placed a distance away from the beam and essentially detects the scattered light. Care must be taken in order not to damage the photodetector. The photodiode used can be seen in figure 5.4



Figure 5.4: PhotoDiode used

With this detector, the pulse width was measured as 25 ns (using the FWHM

definition). The scope output can be seen in figure 5.5

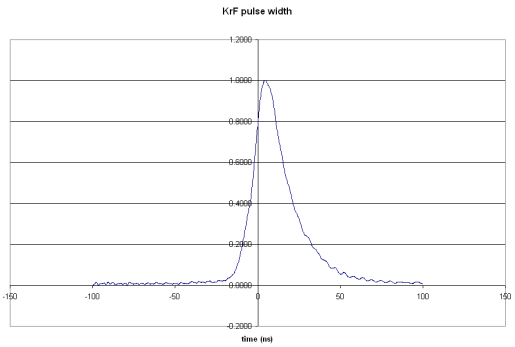


Figure 5.5: PhotoDiode used

The next task was to align the optics in such a way that the laser beam will be directed and focused in the region between the two electrodes. To do this, 2 mirrors and a lens were used. Two different lenses were used: A 75 mm and a 100 mm lens. By using two different lenses, the spot size can be varied. It would be interested to see if the spot size does have an effect on the breakdown process. The basic optics setup can be seen in figure 5.6

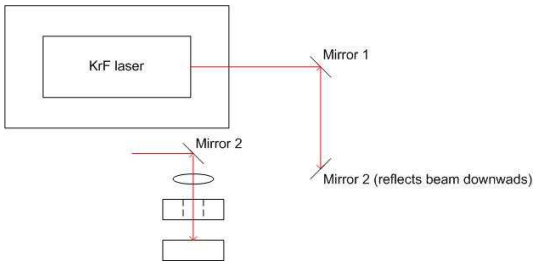


Figure 5.6: Optics setup for KrF laser

Problems with focusing were anticipated since cylindrical lenses were unavailable. For this reason the beam path was made as large as possible in order to allow more light to arrive on the focusing lens. The divergence of a beam produced by an excimer laser is relatively large. The lens was placed in such a position in order to allow the beam to be focused half way between the two electrodes.

5.3 Results obtained from the KrF laser

Once the laser and the optics were setup, a number of experiments were conducted. The aim of all the experiments was to investigate what parameters are important when dealing with laser triggering of spark gaps. In other words, find the lowest energy, the best lens combination that will provide the largest breakdown voltage range.

The equipment used to conduct these experiments are listed below:

- Lambda Physik LPX 200 Excimer laser (248 nm)
- TDS 360 Tektronix digital scope
- Tektronix P6015A HV AC probe (wide bandwidth)
- Fluke HV DC Probe
- Two 248 nm mirrors, 75 mm and 100 mm lenses
- Molectron J50 energy meter
- Photodiode (to measure pulse width)

The impulse generator was setup with a 5 mm gap and spark gap electrodes arranges in a coaxial geometry. The energy of the laser was monitored by means of a suitable energy detector. This was done due to the fact that the laser used was a gas laser. Gas lasers such as the excimer have the following disadvantage: The laser energy drops with time due to depletion of the gas mixture. Once energy has dropped lower than a certain level, the gas has to be replenished. Usually gas lasts for about 2 weeks.

Before and after each experiment, the laser energy, gap size and type of lens used was recorded. The impulse generator was then charged up to a certain voltage and the laser was fired in the gap. Breakdown in the gap was observed by means of the HV AC Tektronix probe. If no electrical breakdown occured, then the voltage was increased and the laser was fired again. If breakdown occured then the voltage was decreased. In effect, a type of "up-down" test was

performed in order to find the minimum voltage that could be broken down for a specific laser energy. This experiment was performed for both lenses (75 and 100 mm) and for different laser energies. All results were recorded. As mentioned, the laser was operating at a repetition rate of 1 Hz and successful breakdown was defined is the laser was able to breakdown the gap repeatably on the first laser shot.

Another experiment that was conducted, was to determine the maximum voltage that the laser-triggered spark gap can withstand. This voltage together with the minimum (laser-induced) voltage will provide the range of the laser-triggered spark gap. This experiment was conducted by slowly charging the impulse generator and monitoring the charging voltage by means of a multimeter connected to the Fluke HV probe.

5.3.1 Voltage withstand levels

As mentioned, one of the experiments that was performed was to determine the maximum voltage that the laser-triggered spark gap can withstand. It is known that the breakdown strength of air is about 27-30 kV/cm. This means that for a 5 mm gap (0.5 cm) the withstand voltage is expected to be about 15-13.5 kV. The experiments showed that this was in fact true. For a 5 mm gap, it was found that the spark gap could withstand a voltage of about 12-13 kV. The results for three gap sizes (namely 10, 5 and 2.5 mm) can be seen in *table 5.1*

Gap size (mm)	Maximum voltage (kV)
10	20
5	13
2.5	8

Table 5.1: Maximum withstand voltages for various gap sizes

5.3.2 Laser-induced breakdown results

Initially 9 experiments were conducted using various lenses, laser energies and gap lengths. These results can be seen in *table 5.2*

Expeirment #1		**Expeirment #2**		**Expeirment #3**	
Laser Energy:	142 mJ	Laser Energy:	142 mJ	Laser Energy:	89.2 mJ
Gap size:	5 mm	Gap size:	10 mm	Gap size:	5 mm
Lens:	75 mm	Lens:	75 mm	Lens:	75 mm
Voltage (kV)	Breakdown?	Voltage (kV)	Breakdown?	Voltage (kV)	Breakdown?
5	yes	11	yes	6	yes
4	yes	10	yes	5.6	yes
1	no	9	no	4	no
Expeirment #4		**Expeirment #5**		**Expeirment #6**	
Laser Energy:	63 mJ	Laser Energy:	40 mJ	Laser Energy:	216 mJ
Gap size:	5 mm	Gap size:	5 mm	Gap size:	5 mm
Lens:	100 mm	Lens:	100 mm	Lens:	100 mm
Voltage (kV)	Breakdown?	Voltage (kV)	Breakdown?	Voltage (kV)	Breakdown?
5.6	yes	8	yes	3	yes
5	yes	7.6	yes	2	yes
4	no	6	no	1	no (questionable)
Expeirment #7		**Expeirment #8**		**Expeirment #9**	
Laser Energy:	202 mJ	Laser Energy:	166 mJ	Laser Energy:	166 mJ
Gap size:	10 mm	Gap size:	5 mm	Gap size:	5 mm
Lens:	100 mm	Lens:	75 mm	Lens:	100 mm
Voltage (kV)	Breakdown?	Voltage (kV)	Breakdown?	Voltage (kV)	Breakdown?
9	yes	4	yes	4	yes
8	yes	3.4	yes	3	yes
7	no	2.5	no	2.5	no

Table 5.2: Inital laser-induced breakdown results

From this table, one can see the following:

- In that case of a 5 mm gap and 100 mm focusing lens, it was found that for an energy of 216 mJ/pulse, the lowest voltage that can be triggered, was found to be 2 kV. In this situation, breakdown at 1 kV was also possible, but not repeatable. This means that the overall range for this laser energy was 2 kV to 13 kV (ΔV=11 kV). It was also found that for a very small energy (40 mJ/pulse), the minimum voltage that could be triggered by means of the laser beam was 7.6 kV. This gives a range of ΔV=5.5 kV. This is considerably less than in the previous scenario. As mentioned though, the laser energy was much lower (18.5% of the initial energy (216 mJ). As expected, the breakdown voltage level dropped with increasing laser energy.

- When a 75 mm lens was used (with the same gap size - 5 mm) the results were similar, but it was noted that the breakdown voltage range was slightly smaller. For example, for en energy of 166 mJ, the breakdown voltage for the case of the 100 mm lens was found to be 3 kV, whereas in the case of the 75 mm lens, the voltage was found to be 3.4 kV (a

600 V decrease). This difference can be attributed to the fact that the longer focal creates a lager spark than the 75 mm lens. In this case, the minimum voltage that was triggered, was 5.6 kV. This was for a laser energy of 89.2 mJ.

- Two more experiments were conducted for both lens configurations and for a 10 mm gap. For a laser energy of 142 mJ (and a 75 mm lens), the breakdown voltage was found to be 10 kV compared with a voltage of 3.4 kV in the case of the 5 mm gap with the same lens. With an energy of 202 mJ and a lens of 100 mm, the breakdown voltage was found to be 8 kV.

In general, it was noted that these results obtained were significantly lower than those obtained in 2003 [16]. With an Nd:YAG laser operating at 1064 nm and about 200 mJ per 10 ns pulse, the breakdown voltage range for a 5 mm gap was found to be 600 V to 13 kV (ΔV=12.4 kV). At the same energy and at 248 nm, the largest voltage range that could be obtained was 2 kV to 13 kV (ΔV=11 kV). In other words, the rage was reduced by 1.4 kV. At the onset of the project, it was expected that when using Ultraviolet light, due to the high energy per photon (4.6 eV/photon for the case of 248 nm compared with 1.1 eV/photon in the case of 1064 nm) breakdown in air would be accomplished far easier. The expected result would be an increase in the breakdown range.

When the experiments were conduced, it was noted, that the focused KrF laser beam was not able to ionise air. In other words, the laser was not able to create a spark in air. This came as a surprise due to the high laser and photon energy. This meant that the mechanism that was causing electrical breakdown in the gap was primarily due to electrode ablation. The laser beam is powerful enough to ablate the surface of the electrodes. The result of this is that electrode particles are released and they are in fact aiding in the breakdown process. This is because of the coaxial spark gap arrangement. The fact that the KrF laser was not able to generate a spark in air can be attributed to the following reasons:

First of all, the beam shape is not good. As mentioned, it is rectangular (26×8 mm). This makes the act of focusing the beam difficult. In *figure 5.7*, one can

see the burn pattern produced by the UV laser beam after being focused by the 75 mm lens. It can be seen that the spot produced is still very large. Not large enough to ensure that the power density is high enough.

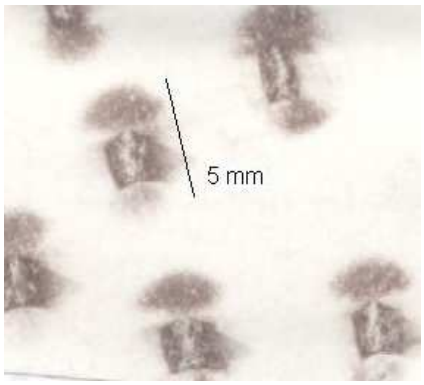


Figure 5.7: Spot size and shape after focusing

Another reason is that the pulse width of the KrF laser is much longer than that of the Nd:YAG. As mentioned, for the excimer, the pulse width was measured to be about 25 nm compared to 8-10 ns for the YAG. This means that once again, the laser beam intensity will be lower. In fact, the resultant intensity can be calculated using the method discussed in chapter 3.

A numerical integration was performed using the time pulse data obtained from the oscilloscope. The spacial profile of the beam was taken from burn pattern obtained. The pattern was approximated to a rectangle with dimensions of 1.3×2.5 mm. This approximation was made by considering the region of highest energy (where ablation on the paper was largest). By performing the integration and using two different values for laser energy: 109 mJ and 167 mJ, the intensities obtained were 118 MW/cm^2 and 180 MW/cm^2. These two power densities are very much lower than the required value of 100 GW/cm^2 according to literature [11]. It can be said that this is the reason why the laser was not able to cause ionisation in air. It is interesting though, that even at such a low power density, the breakdown voltage range proved to be quite wide (2 kV to 13 kV for an energy of 216 mJ to 233 MW/cm^2).

5.3.3 Pre-breakdown phenomena

For the cases where breakdown did not occur, the volts/division of the scope were reduced significantly (to a couple of volts/division). In this range, it was noted that when the laser was fired, a very small impulse voltage appeared on the output. The detected signal's amplitude was in the region of couple of volts. As the voltage across the gap increased, the amplitude of the output wave increased. At some point, the amplitude increased dramatically, indicating that the gap had indeed broken down. Measurements were taken for various combinations of lenses, laser energies and gap lengths. Three different gap lengths were tested, these being 2.5 mm, 5 and 10 mm. The tables obtained from these experiments can be seen in *Appendix C*. A graph was plotted for a set laser energy (169 mJ/pulse), a 75 mm lens and for the three above mentioned spark gap lengths. This plot can be seen in *figure 5.8* The experimental set up in this case, was a high voltage probe at the output of the impulse generator feeding data to the oscilloscope. The spark gap arrangement was kept the same,in terms of electrode orientation and configuration.

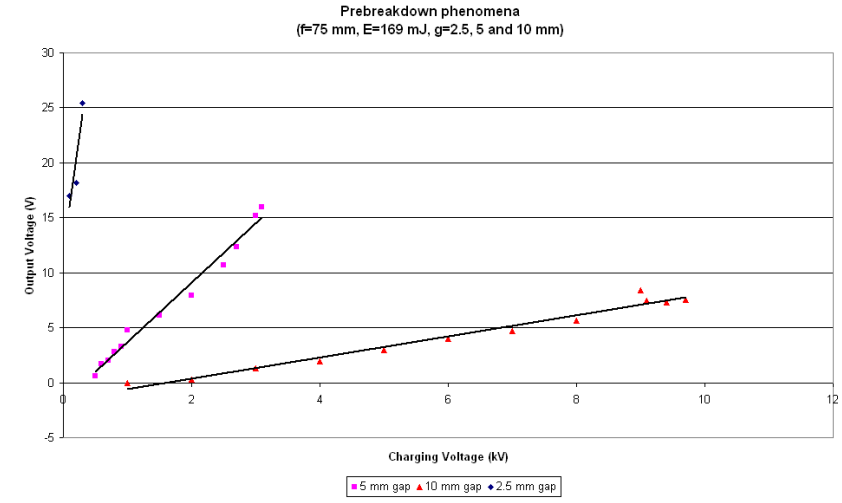


Figure 5.8: Plots of the input and output voltages for thee different gap lengths

In these plots, it must be noted that the last point plotted indicates the last measurement before electrical breakdown is in fact observed. It can be seen that as the input voltage increases, the output voltage also in its turn increases. What is more, this variation is linear. For the shortest of the three gaps (2.5 mm), the slope was found to be very high (42) indicating that breakdown was

achieved very quickly. In fact, for this gap, the minimum voltage that was successfully triggered was approximately 400 V. In the case of the 5 mm gap, breakdown occured much later. This is verified by the fact that the gradient of the straight line was much less (5.1 - about 12% of the inital gradient). Finally, for the case of the 10 mm gap, the gradient was found to be very small (0.94 - 2% of the inital slope). For each case, the equation of the straight line was evaluated and the following was found:

- For the 2.5 mm gap: $V_{out} = 42V_{in} + 12.8$
- For the 5 mm gap: $V_{out} = 5.1V_{in} - 1.53$
- For the 10 mm gap: $V_{out} = 0.94V_{in} - 1.56$

It must be noted that the resultant prebreakdown impulse was approximately a 20/400 μs impulse compared to the 0.5/400 impulse normally produced by the generator. The waveform of this impulse can be seen in *figure 5.9*

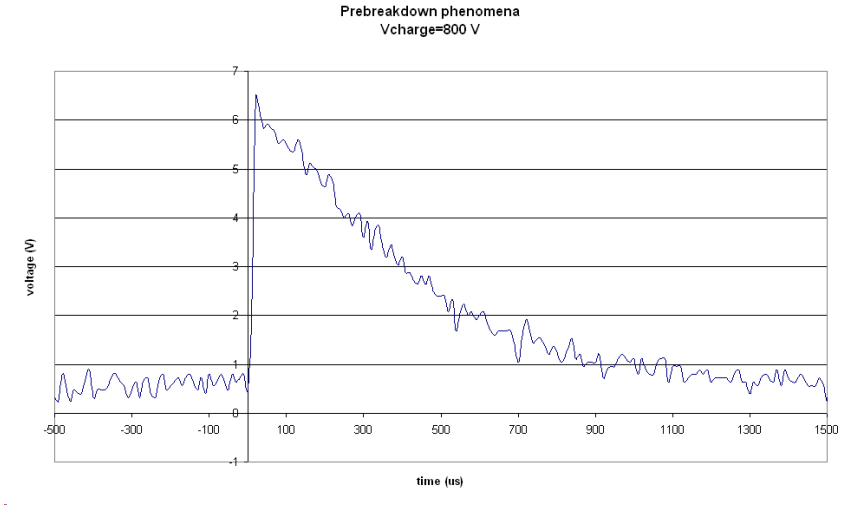


Figure 5.9: Plot of the prebreakdown impulse for a charging voltage of 800 V

An explanation of these phenomena, can come form considering the formation of space charges [6]. The formation of space charges can be explained by considering a severe case of two electrodes, a spike opposite a plain. The spike is the anode and the plain is the cathode. A voltage is applied across the gap. This configuration can be seen in *figure 5.10*

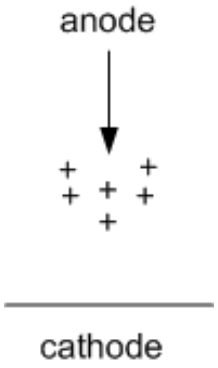


Figure 5.10: Creation of space charge between a point and a plain

In a situation as described above, the electric field at the point of the anode is very high. This results in electrons being drawn away from the surrounding gas and absorbed by into the anode. The result is the formation of a positive space charge around the tip of the anode. Under DC conditions, this space charge can remain uncharged for large periods of time. As the voltage across the gap increases though, discharges start developing, These discharges are of short duration. The frequency with which these occur increases with increasing voltage. When the voltage becomes sufficiently high, breakdown across the gap occurs.

It can be said, that a similar phenomenon occurs in the laser triggering experiments. As mentioned, for a small charging voltage (600-800 V), impulses of low amplitude (from as low as 1 V to as high as 27 V) appear at the output of the impulse generator. Since the laser beam is striking the anode, it can be said that due to the high laser beam intensity, a local space charge is generated at the anode (due to air ionisation and electrode ablation).

5.3.4 Beam quality improvement

In view of the results obtained, an effort was made to improve the quality of the KrF laser beam. The aim was to ultimately increase the power density making it easier for air to become ionised. The first strategy that was adopted, was to use lens combinations. When using two lenses, the focal length is dependent on the focal length of the two lenses and their separation [24].

$$\frac{1}{f} = \frac{1}{f_1} + \frac{1}{f_2} - \frac{d}{f_1 f_2} \tag{5.1}$$

where f_1 and f_2 are the focal lengths of the lenses used and d is the lens separation.

This method did not provide good results. This was because of the beam shape and the inability to centre the lenses accuratetely.

Another method would be to try and shape the laser beam by using the technique seen in *figure 5.11*:

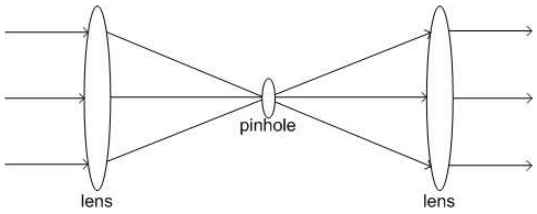


Figure 5.11: Reconstruction of laser beam by using a lens-pinhole combination

The principle of operation of this beam-reshaping technique is that a pinhole of the desired shape is placed at the focus of the beam. The focal length will be dependant on the lens used. The beam then will be allowed to diverge and the second lens will reproduce the now shaped beam. This method is difficult to implement since precise placement of the components is required and also by using a pinhole, a large amount of energy will be lost. The same applies for the case of a pinhole placed directly in front of the laser beam.

The best technique to use would be to increase the size of the laser beam that is incident on the lens. This can be done by allowing the laser beam to travel along a longer path. A 4 m path was created was can be seen in *figure 5.12*

Both a 2 m concave and a flat mirror was used for mirror 2 in *figure 5.12*. In both cases, breakdown in air was not achieved. In *figure 5.13*, the burn patterns produced by the laser beam at each mirror until the beam is focuses in the gap.

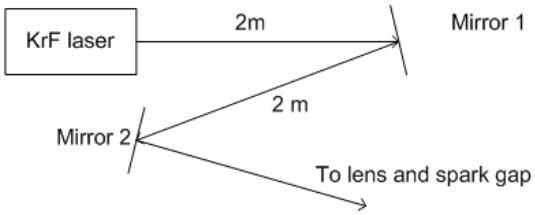


Figure 5.12: Use of mirrors to create a larger laser beam profile

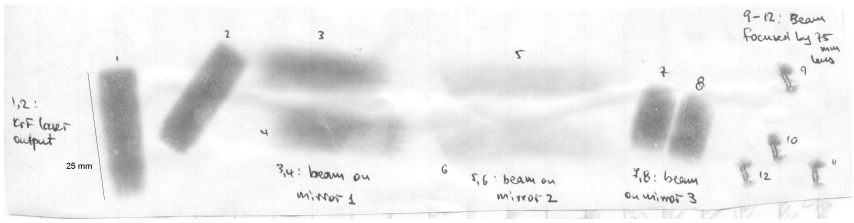


Figure 5.13: Burn patterns produced by excimer with multiple mirrors

5.4 Conclusion

In this chapter, a KrF excimer laser was used. The results obtained were not as expected. The fact that the laser was operating in the UV range was not sufficient to cause visible ionisation in air. For three different gaps and two different energies, the voltage breakdown ranges were found to be as follows: 800 V to 6 kV for a 2.5 mm gap, 3kV to 12 kV for a 5 mm gap and 10 kV to 20 kV for a 10 mm gap. This was for an energy of 250 mJ per pulse. When the energy was reduced to 100 mJ, the minimum voltages obtained were 3 kV, 5.6 kV and 10 kV for the 2.5, 5 and 10 mm gap respectively. When breakdown did not occur, it was noticed that a very small amplitude impulse appeared on the output. This impulse was faster than the breakdown impulse voltage and could be attributed to the formation of a space charge when the laser bream interacts with the anode. From these experiments it can be concluded that the beam quality and focusing strategy is very important. In the next chapter, the experiments conducted with the Nd:YAG laser will be presented. A YAG laser operating at 1064 (near IR), 532 (green) and 355 nm (UV) was used in order to compare the results obtained with the excimer. In essence the YAG will be used to determine to an extent, the effects of wavelength on laser-induced breakdown.

Chapter 6

Experiments with the Nd:YAG laser

6.1 Introduction

In the previous chapter, the performance of a KrF excimer laser was presented. Even though the laser was operating in the UV frequency range (248 nm), the resultant breakdown voltage ranges were not as wide as expected. Experiments done with a YAG laser operating at 1064 nm showed that the minimum voltage that could be broken down was 600 V. It was expected that by using UV instead of IR light, the range could be reduced even more. This is why a YAG laser was used. The laser was operating at all three wavelengths (1064, 532 and 355 nm). The energy output of the laser was approximately 170 mJ and the pulse width was 8 to 10 ns. The same experiments are to be conducted and the results compared with those obtained with the KrF laser. In effect, through this exercise, the wavelength dependence of the laser-induced breakdown can be examined. The same spark gap and the same impulse generator were used for these experiments.

6.2 The Nd:YAG laser

Unlike the excimer, the Nd:YAG laser is a solid state laser. It operates by optically pumping the YAG crystal with high intensity flash lamps. The YAG

laser is able to produce a Gaussian beam with high peak power. The pulse width of the YAG laser is also much shorter than the excimer: 8 to 10 ns compared with 25 ns for the KrF. The wavelengths that will be used are:

- 1064 nm - near infrared
- 532 nm - green light
- 355 nm - ultraviolet

It must be noted that special care must be taken when operating a laser like the YAG. This is because the combination of wavelength and high beam intensity can be very harmful to the human eye. Wavelengths from 1400 nm to 400 nm get focused on the retina and can cause severe damage. The laser that was used was a Continuum located at the National Laser Centre in Pretoria. The laser can be seen in *figure 6.1*



Figure 6.1: The Nd:YAG laser used in the experiments

The equipment that was used can be seen below:

- Continuum Nd:YAG laser (1064, 532, 355 nm)
- Two TDS 360 Tektronix digital scopes
- Tektronix P6015A HV AC probe (wide bandwidth)
- Fluke HV DC Probe

- mirrors coated for all three wavelengths and 100 mm lenses
- Molectron J50 energy meter
- Photodiode (to measure pulse width)

Throughout all the experiments, the energy and pulse width of the laser was monitored in order to ensure that these parameters do not change and thus influence the results obtained.

When the laser was set up, the energy and pulse width were measure to ensure that the laser operates correctly. The energy output was varied by adjusting the Q-switch. The laser was set up to operate at its fundamental wavelength (1064 nm). Because the laser has a very high peak power, care was taken not to damage the energy meter used. This was done by introducing a filter between the beam and the meter. The transmittance factor of the filter was found by taking readings with and without the filter at low energy. The calibration table that was drawn up can be seen in *table 6.1*

Qswitch (us)	E' (with filer - mJ)	E (without filter - mJ)	Ratio (E'/E
90	3	21	0.16
92	7	27	0.25
94	8	32	0.25
96	9	38	0.25
98	11	42	0.26
100	12	48	0.25
105	18	76	0.24

Table 6.1: Calibration table for the energy meter filter at 1064 nm

From this table is an be calculated that the average ratio was 0.24. In other words, to obtain the total energy of the pulse, one has to divide the transmitted energy through the filter by this factor (0.24). From these measurements it was found that for 1064 nm, the maximum energy output was found to be 216 mJ at a Q-switch value of 150 μs

The pulse width was measured by means of the photodiode. The pulse that was obtained can be seen in *figure 6.2*

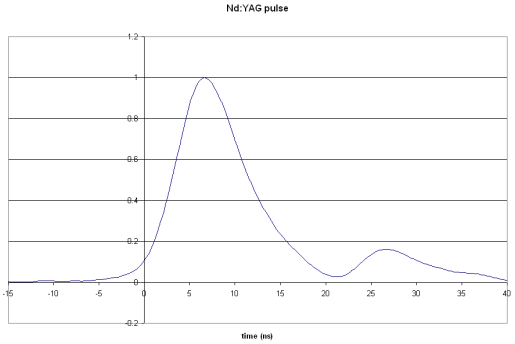


Figure 6.2: The Nd:YAG laser pulse obtained

Once again, in order to record the pulse width, the laser beam was allowed to strike a non-reflective surface such as polystyrene or cardboard. The photodiode was placed a distance away from the beamstop in order to avoid optical flooding of the detector. From this plot, one can see that the pulse width (FWHM) is between 8 and 10 ns.

Heat sensitive paper (fax paper) was once again used to get an idea of the beam profile. The burn mark showed that the laser beam coming out of the laser had a gaussian profile (as expected) with a diameter of about 3 mm. The burn patters obtained can be seen in *figure 6.3*



Figure 6.3: Burn pattern of YAG laser

When a 100 mm lens was used to focus the beam, the spot size was found to be about 0.4 mm (400 microns). The focused beam can be seen in *figure 6.3* just below the pattern marked with the 3 mm indicator.

Using a spot size of 400 microns, a laser energy of 216 mJ (at maximum Q-switch) and using the pulse width data obtained from the oscilloscope, the laser beam intensity was evaluated to about 51 GW/cm^2. Under these conditions, breakdown in air was observed. In other words, the laser beam was able to break down unbiased air at the focal point of the lens. This is important since the KrF laser was not able to cause ionisation in air at the same energy and using the same type of lens. The reason for this was, as mentioned, the low laser beam intensity (long pulse width and large spot size).

6.3 Laser breakdown experiments

6.3.1 Experiment at 1064 nm (near infrared)

The impulse generator was set up with a spark gap of 5 mm. The gap was arranged once more in a coaxial geometry. A 100 mm focusing lens was used. The lens was positioned in such a way as to ensure that its focal point is located half way between the two electrodes.

The first step was to see at what energy breakdown in unbiased air occured. By adjusting the Q-switch of the laser it was found that 70 mJ was the lowest energy that the laser was able to cause ionisation in air. Following this, two experiments were conducted, one at a relatively high energy (142 mJ) and the other at a lower energy (102 mJ). The following results were observed:

Experiment #1		**Expeirment #2**	
Laser Energy:	142 mJ	Laser Energy:	102 mJ
Gap size:	5 mm	Gap size:	5 mm
Lens:	100 mm	Lens:	100 mm
Charging Voltage	Breakdown ?	Charging Voltage	Breakdown ?
2	yes	4	yes
1	yes	3	yes
600	yes	2.5	yes
500	no	2	no

Table 6.2: Breakdown results for 1064 nm

From the results in table 6.2, it can be seen that for an energy of 142 mJ per pulse, the laser was able to breakdown a voltage as small as 600 V. This is very significant. The first important point is that this results correlates with the work done in 2003 [16]. In this work, it was noted that for a laser energy of 230 mJ per pulse (for a Continuum Surelite YAG laser) the minimum breakdown voltage that was achieved was 600 V for a 5 mm air gap. This shows repeatability of the result. The other very significant point is that the excimer was unable to breakdown such a low voltage even with the same amount of output energy per pulse. It was also noted that for a lower energy of 102 mJ, the minimum breakdown voltage achieved was about 2.5 kV.

6.3.2 Experiments at 532 nm (green light)

Once results were obtained from the laser operating at 1064 nm, the first harmonic oscillator crystal was inserted. This enabled the laser to emit a beam in the green region of the spectrum (532 nm). The same setup was used. The only difference was the use of lenses and mirrors coated for 532 nm. Once again, a 100 mm focusing lens was used.

The fist point to check with the new laser setup, were the laser parameters (spot size, laser energy and pulse width). Fax paper was used to estimate the spot size before and after focusing and a photodiode was used to determine the pulse width. The pulse width as found to be between 8 and 10 ns (as expected). The burn pattern can be seen in figure 6.4

From *figure 6.4* it can be seen that the beam size is about 3 mm in diameter. The spot size is again very small. It was measured to be about 400 microns (at the focal point)

As far as the energy is concerned, the an energy meter was used in the same way as described in the previous section. Because the energy emitted by the laser, a filter was needed when measuring the energy output. The lowest energy that was measured was about 1.2 mJ and the highest was about 40 mJ at a Q-switch value of 150 μs

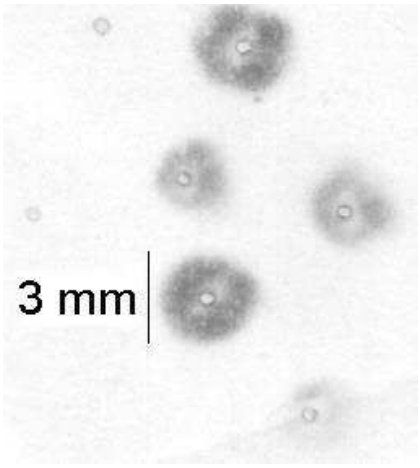


Figure 6.4: Burn pattern of YAG laser at 532 nm

The first experiment that was conducted, was the determination of the energy required to breakdown unbiased air. The laser beam was allowed to be focused by the 100 mm lens in a region away from the spark gap. (to achieve unbiased air). The experiment showed that air broke down successfully at an energy of 26 mJ. This result is quite interesting since for the case of the 1064 nm beam, the minimum energy required to generate a spark in air was approximately 70 mJ. This shows that these could be a wavelength dependence in the laser-induced breakdown mechanism in air.

Once these initial experiments/tests were conducted, the electrical breakdown of the impulse generator spark gap was investigated. A 5 mm gap was set up and the 100 mm lens was placed in such a way, that the focal point was mid way between the two electrodes (electrodes were arranged in a coaxial geometry as before). The laser was operating at optimal Q-switch (150 μs). As before, one laser pulse was fired in the gap, and breakdown status was observed by means of the presence (or not) of the breakdown waveform on the oscilloscope.

The results obtained were interesting. The results obtained can be seen in *table 6.3*

Gap: 5mm	
f=100 mm	
E=37.6 mJ	
Charging Voltage	Breakdown ?
6	yes
5	yes
4	yes
3.6	yes
3	no

Table 6.3: Laser-induced breakdown voltages

From this *table (6.3*, it can be seen that for an energy of 40 mJ (37.6 mJ), the laser was able to break down a voltage of 3.6 kV. This result is very interesting when compared to the results obtained with the KrF excimer laser. In the case of the excimer, the same breakdown voltage was obtained with an energy of about 200 mJ. This can be explained by means of power density calculations. In the case of the YAG laser, the beam is Gaussian (circular burn pattern). This means that it is easier to focus and results in a very small spot size (400 microns in diameter. The power density can be calculated to about 9.3 GW/cm^2 (for an energy of 40 mJ). In the case of the excimer, the power density can be estimated to be about 43 MW/cm^2. The fact that the intensity of the KrF laser is so low compared to the YAG is because of the rectangular beam produced by the former.

The final experiment that was conducted involved looking at the minimum voltage that was able to be triggered by a range of laser energies (at 532 nm). By plotting the breakdown voltage in kV versus the output laser energy, the following plot (*figure 6.5*) was obtained:

In *figure 6.5* it can be see that as the laser energy increases, as expected, the breakdown voltage decreases. It is can be noted though, that as the experiment progresses, the change in breakdown voltage becomes smaller. The trend noted is that the breakdown voltage decreases and aproaches a certain limit asymptotically. This is quite interesting considering that the variation in laser energy with increasing Q-switch is nearly linear as can be seen in *figure 6.6*.

This voltage limit would be primarily dependant on the gap length and the laser energy. If the laser were able to output a higher laser energy, then the voltage limit would be smaller. This voltage though would still be reached

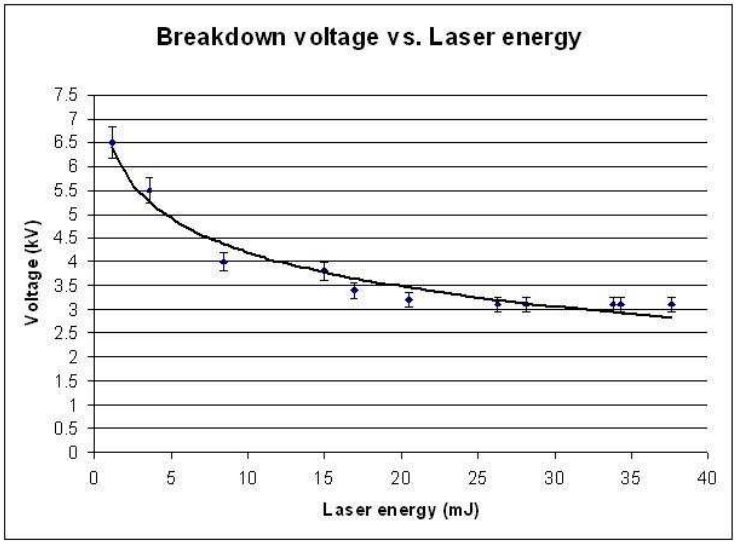


Figure 6.5: Variation of breakdown voltage as laser energy is altered

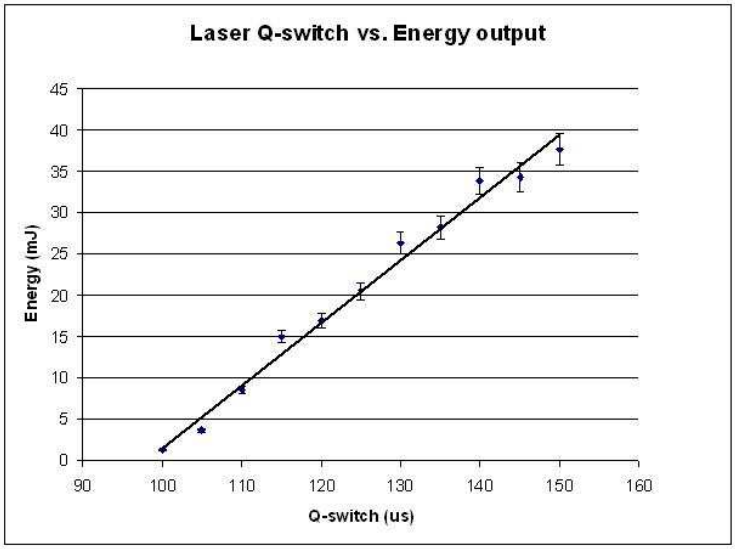


Figure 6.6: Variation of laser energy with varying Q-switch value

asymptotically. This phenomenon can be explained be considering the fact that for each spark gap and laser energy arrangement, there is a minimum voltage that can be broken down.

6.3.3 Experiments at 355 nm (Ultraviolet)

Once the experiments at the 532 nm were concluded, the second harmonic oscillator was inserted in the laser so that the wavelength output would be at 355 nm (ultraviolet). As before, the laser was tested in order to see whether the laser parameters are as expected.

As before, an energy meter was used to measure the energy output of the laser. Once again, the use of a filter to attenuate the beam energy was not necessary (low energy output). Measurements showed that the laser was able to output a minimum of 0.6 mJ and a maximum of about 7 mJ (at a Q-switch of 150 μs). The pulse width was also verified to be in the expected range of 8 to 10 ns.

The impulse generator was once again set up with a 5 mm gap and suitable focusing and steering optics. Calcium Fluoride optics were used since the light emitted was in the UV range. A 100 mm lens was used to focus the beam. The laser was operating at 1 Hz repetition rate. Voltage was applied to the gap, but it was noted, that the laser was not able to break down the gap under any voltage. This can be attributed to the fact that the laser beam intensity (and energy) was not high enough.

6.4 Conclusion

In this chapter, breakdown experiments using an Nd:YAG laser were described. The laser was operating at 1064, 532 and 355 nm. Throughout all the experiments, a 100 mm focusing lens was used. The spot size obtained in all three cases was found to be about 400 microns. The laser was able to produce an energy of about 170 mJ at 1064 nm, 40 mJ at 532 and 7 mJ at 355 nm. The laser-induced breakdown experiments showed that when the laser was operating at 1064 nm, the breakdown voltage was found to be 600 V for an energy of 142 mJ per pulse. For an energy of 102 mJ, the breakdown voltage obtained, was found to be 2.5 kV. When the laser operated at 532 nm, the minimum breakdown voltage obtained for 40 mJ, was 3.6 kV. In the case of 355 nm, the

energy was not enough to breakdown the 5 mm gap used. These results show that the ability of a laser to cause electrical breakdown is dependant on the beam intensity (power density) and to an extent on the wavelength. It was found that the laser was able to generate a spark in air for a power density of about 10 GW/cm^2

Chapter 7

Laser breakdown in sulphur hexafluride (SF_6)

7.1 Introduction

In the previous chapter, the used of an Nd:YAG laser to cause breakdown in air was presented. The laser was able to operate at its thee harmonics (1064, 532 and 355 nm). In these experiments, air at standard temperature and pressure conditions was used as the gap atmosphere. In this experiment, laser-induced breakdown in gases other than air, will be presented. In the experiments, the gas sulphur hexafluoride was used. The temperature of the gas was maintained at room temperature. The gas pressure though was varied from -60 kPa to 60 kPa. The laser that was used for these experiments was once again the KrF excimer. SF_6 is a highly electronegative gas. It is used as an insulating gas in many High voltage applications. However, if the electric field exceeds a certain value, breakdown in the gas is inevitable. In SF_6, the breakdown process occurs more dramatically than in air. In other words, it is expected that the laser beam will be able to cause breakdown in SF_6 relatively easier (than in air). In this chapter, the design of the pressurised spark gap used will be presented. The experiments that were conduced will be described and the results discussed.

7.2 The spark gap used

In order to conduct experiments performed under pressure, a suitable spark gap was designed. The requirements were as follows:

- The container should be able to withstand pressures from vacuum to about 60 kPA (above atmospheric) for a long period of time (the container must be well sealed)
- The container must be able to accommodate the two high voltage electrodes in a coaxial geometry
- There must be an entrance for the laser beam (a high transmittance window for UV)
- Means of drawing a vacuum and inserting a gas must be present

In *Appendix D*, one can find an engineering drawing of the spark gap that was designed. A simple drawing (not to scale) of the main container of the spark gap, can be seen in *figure 7.1* (all dimensions in mm). The view is a section in the y-direction

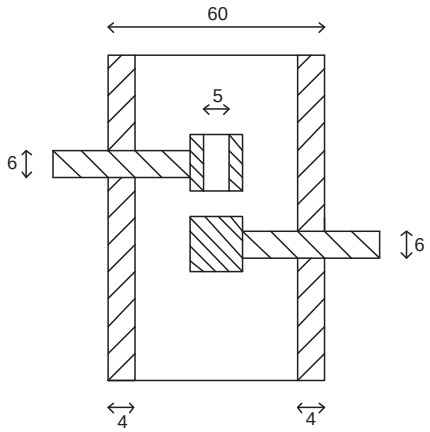


Figure 7.1: A simple drawing of the SF_6 spark gap

Taking these requirements into consideration, materials were chosen for the construction of the air-tight container. Perspex tube of outer diameter of 60 mm and wall thickness of 4 mm was used as the main part of the spark gap

casing. Perspex was used in order to make aligning the laser beam easier due to the fact that perspex is transparent. A 4 mm wall thickness was chosen for two reasons, the first being strength. A thicker container translates to better withstand to pressure. When mounting the electrodes, the extra wall thickness will allow better sealing ability (more threads will be able to be created).

As can be seen from *figure 7.1*, the electrodes were mounted by means of 6 mm threaded rods. The electrodes themselves, were machined out of brass. As in the other experiments, their profile was cylindrical and hole was bored down the axis of the cathode. The hole was 5 mm in diameter - enough to allow the focused KrF beam into the region of the gap without clipping occuring.

In order to allow the laser beam into the region of the gap, a suitable window that would be able to allow UV light to be transmitted through it, was needed. Quartz is one such substance. A quartz window was not available, in which case, a Calcium Fluoride (CaF) window was used. The window had a 1 inch diameter and had a 2 mm thickness. The window was secured in place by means of epoxy.

When the gap was assembled, rubber seals were placed between the container edges and the top and bottom lids. At the same time, a pressure gauge (-100 to 300 kPa) and a tap were installed. The tap would be able to keep the container sealed once a vacuum is drawn, or when SF_6 will be present in the container under pressure. A suitable pump was used to draw the necessary vacuum.

7.3 Breakdown experiments

Once the spark gap was built and tested, it was taken together with a bottle of SF_6 to the NLC. Once again, the KrF excimer laser was set up. Again, the pulse width and energy were tested. The optics that were used included a 45 degree steering mirror and a 100 mm focusing lens. The optics were aligned in such a way, that the laser beam would be able to enter through the hole in

the cathode and strike the surface of the anode. The energy of the laser was monitored constantly in order to make sure that it did not change.

In the experiments, 5 different pressures were used: -60 (air vacuum), -40 (SF_6), -20 (SF_6), 0 (atmospheric SF_6), and 20 kPa (SF_6). The laser was operating at 200 mJ per 25 ns pulse, a 100 mm lens and a 5 mm gap was used.

- Experiment 1: -60 kPa (0.4 bar absolute) vacuum. In this case, the vacuum pump was used to extract as much air from the container as possible, without adding SF_6. The gap was then connected to the impulse generator, and the usual voltage breakdown tests were conducted. It was found that the minimum breakdown voltage the laser was able to trigger was 2 kV
- Experiment 2: -40 kPa (0.6 bar absolute) SF_6. Here, once the air was removed from the container, a quantity of SF_6 was added, until the pressure gauge indicated that the container pressure was -40 kPa. In this case, the minimum breakdown voltage was found to be 3 kV
- Experiment 3: -20 kPa (0.8 bar absolute) SF_6. The pressure was increased to -20 kPa by adding more sulphur hexafluoride. The same process was repeated, and the breakdown voltage was found to be 5 kV.
- Experiment 4: SF_6 at atmospheric pressure (1 bar). In this situation, as expected, the minimum breakdown voltage that the laser was able to trigger was found to be much higher than in the previous 3 scenarios. It was observed that the laser was able to trigger 8.5 kV
- Experiment 5: SF_6 at 20 kPa (1.2 bar). In this experiment, it was observed that the breakdown voltage increased dramatically to 10 kV for the 5 mm gap

The above mentioned results can be summarised in the plot seen in *figure 7.2*.

The experiments showed an expected trend: As the pressure of the gas in the spark gap container increased, the minimum voltage that the laser is able to breakdown also increased. It is interesting to compare the plot obtained above

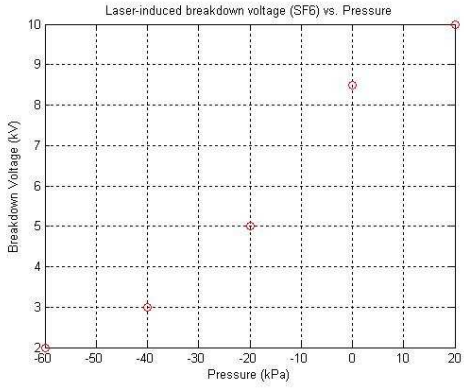


Figure 7.2: Plot of breakdown voltage in SF_6 vs. spark gap pressure

with that of the Paschen curve for the pd product used. The pressure in the vessel varied from 0.4 to 1.2 bar (absolute). Plotting the two graphs (*figure 7.3*), showed the following:

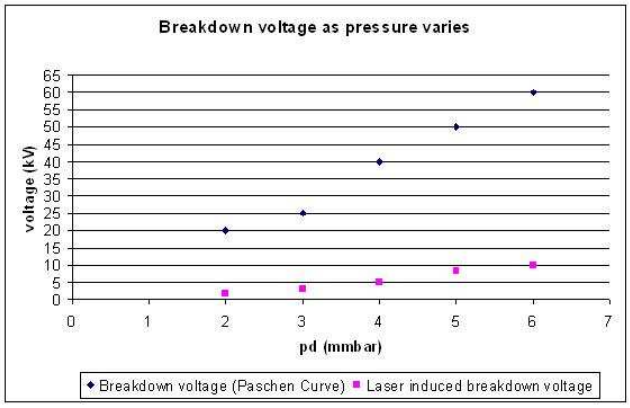


Figure 7.3: Comparing the breakdown voltages obtained from Paschen Curve with the laser-triggered voltages

From *figure 7.3*, it can be seen that the laser-triggered voltages follow a very similar pattern to that of the Paschen curve [25]. It was noted though that the average "gradient" of the laser triggered "Paschen curve" was less than the proper curve. This can be attributed to to parameters: First of all, the vacuum pump was not able to produce a perfect vacuum. The second reason is that the laser was able to reduce the breakdown voltage for each pd combination. This can be seen by considering the fact that the laser triggered "Paschen curve"starts at a much lower value.

7.4 Conclusion

In this chapter, the laser-induced breakdown process in sulphur hexafluoride (SF_6) was investigated. A 5 mm gap was placed in an airtight container and connected to the impulse generator used in all the previous experiments. A calcium fluoride (CaF) window was used to allow the UV laser beam to enter the container. The beam was produced by the Lambda Physik Excimer laser (KrF - 248 nm). A 100 mm focusing lens was used. The experiments showed that the focused laser beam (200 mJ per pulse) was able to break down SF_6 at various pressures ranging from 0.4 to 1.2 bar (absolute). For a pressure of 0.6 bar, the laser was able to breakdown a minimum of 2 kV, 3 kV, 5 kV and 10 kV for pressures of 0.4, 0.6, 0.8, 1 and 1.2 bar respectively. The maximum withstand voltages (as obtained from the SF_6 Paschen curve) for each combination of pressure and gap length were 20 kV, 25 kV, 40 kV, 50 kV and 60 kV respectively for the above mentioned pressures. This shows that the laser-induced breakdown voltage is on average 14% of the maximum withstand voltage.

Chapter 8

The summing up

In this thesis, laser-induced breakdown (electrical breakdown) in spark gaps was investigated. In particular, UV laser light was used. In the experiments, two lasers were used. The UV laser was a KrF Excimer (248 nm) operating at about 230 mJ per 25 ns pulse. The laser produced a rectangular laser pulse (26 *times* 8 mm). The second laser used was a Q-switched Nd:YAG laser. This laser was able to emit light in the near infrared region (1064 nm), in the green (532 nm) and UV (355 nm) region of the spectrum. The YAG laser was able to output a maximum energy of 170 mJ at 1064 nm, 40 mJ at 532 and 10 mJ at 355 nm. Pulse width in this case was 8-10 ns. The laser beam was gaussian and thus easy to focus. In all experiments, the same electrodes were used (5 mm or 10 mm gap). The spark gap electrodes were set up in a coaxial configuration (beam parallel to the axix of the gap). The focusing lens that was used was a 100 mm lens with a suitable coating for each wavelength.

In the case of the KrF laser, it was found that the laser was able to trigger a minimum voltage of 2 kV for an energy of 216 mJ per pulse (for a 5 mm gap). This is approximately 13.6% of the breakdown voltage according to the Paschen curve for air (5 mm gap, 1 bar). For a very low energy (40 mJ) and same gap setup, the breakdown voltage was found to be 7.6 kV (40% of the breakdown voltage). By using a 75 mm lens (instead of a 100 mm lens), the breakdown voltage was found to be higher 3.4 kV compared with 3 kV in the case of the 10 mm lens (for an energy of 166 mJ). This can be explained by considering that in the case of the 100 mm lens, the spark generated is larger than in the case of the 75 mm focusing lens. When a 10 mm gap was used (for

an energy of 142 mJ, 75 mm lens), the breakdown voltage obtained was found to be 10 kV (35.2% of breakdown voltage in air).In the case of a smaller gap (5 mm), the laser was able to trigger a voltage of 4 kV (27% of breakdown voltage).

During the experiments is was noted that for a very low charging voltage, when the laser was fired in the gap, a very small in amplitude ranging from a couple of volts to about 10-20 V appeared on the output of the generator. The waveform was slightly faster (20/400 μs) than the correct impulse voltage (1.7/1200 μs). These "prebreakdown phenomena" can be attributed to the fact that the laser is able to generate a space charge in the region of the gap. From this space charge, discharges start developing, These discharges are of short duration. The frequency with which these occur increases with increasing voltage. as the voltage across the gap increased, the amplitude of these "discharges" increased until at some point, breakdown of the gap occured. This increase of amplitude was found to be linear. For a short gap, the voltage at which breakdown happend was attained far quicker than in the case of a longer gap.

The main problem that was identified, was that the KrF laser was not able to create ionisation in air. In other words, the focused laser beam was not able to generate a spark in unbiased air at the focal point. This can be attributed to the fact that the laser beam was not able to be focused in a tight enough spot. The power density required to generate a spark in air is about 10 GW/cm^2. The KrF laser beam intensity was calculated to about 230 MW/cm^2. The problem also lies in the fact that the pulse width of the laser is relatively long.

In view of the results obtained with the KrF laser, an Nd:YAG laser was used to investigate laser triggering of spark gaps. The advantage of the YAG laser is high peak power (gaussian pulse), ease of focusing and short pulse width (8-10 ns). The laser was set up initially to operate at 1064 nm (infrared). Under these conditions and for a 5 mm gap, a 100 mm lens and a pulse energy of 142 mJ, the minimum voltage that could be broken down, was found to be 0.6 kV (4.1% of the breakdown voltage in air). For an energy of 102 mJ, the voltage was found to be 2.5 kV (17% of breakdown voltage). The beam had a 400 micron diameter at the focal point and the power density was calculated to be

about 33 GW/cm^2. Breakdown of unbiased air occured at an energy of about 70 mJ (16 GW/cm^2.

When the wavelength was changed to 532 nm (green light), the minimum voltage that the laser was able to trigger, was found to be 3 kV. This was for a maximum energy of 40 mJ per pulse. In the case of green light, breakdown in air occured when the energy was set to 26 mJ. This shows that in this case, the wavelength of the laser beam does indeed play a role in laser-induced electrical breakdown. The energy required to cause ionisation in air, dropped from 70 mJ in the case of infrared, to 26 mJ in for 532 nm. When the laser was set up for operation at 355 nm, it was found the the maximum energy (10 mJ) was far too low to give any meaningful results.

Finally, laser-induced breakdown was investigated for the case where the spark gap is placed in an atmopshere other than air. Sulphur hexafluoride was selected as the gap atmosphere. A suitable airtight vessel was designed to contain the gas. The gas pressure was varied from as low as 0.4 bar to as high as 1.2 bar. The results showed that, as expected, for increasing pressure, the minimum voltage that can be broken down increased. For 5 different pressures: 0.4, 0.6, 0.8, 1, 1.2 bar, the laser was able to trigger voltages of maginudes: 2, 3, 5, 8.5, and 10 kV respectively. These voltages are equivalent to a percentage of 10, 12, 12.5, 17 and 16.7% of the breakdown strength of SF_6 for each respective pressure.

By considering all the above, the following summing up statements can be made:

- The beam quality and the resultant laser beam intensity (power density) is very important in laser triggering of high voltages
- The type of lens used (in terms of focal length) does have an impact on laser breakdown. The lens that yielded the best results was found to be a 100 mm lens.
- The wavelength of the beam does indeed influence the breakdown results. In theory, the shorter the wavelength, the higher the photon energy and

the easier ionisation occurs. However, it is not a very important parameter compared to power density.

- SF_6 seems to be a better gas to use for the laser-triggered spark gap atmosphere. This can be seen from the fact that when SF_6 was used, the laser was able to trigger voltages that represented low percentages of the breakdown strength of this gas (from as low as 10% to 16.7%). This is represents a better performance that that of pure air.

References

[1] S.C. Haydon. *An introduction to discharge and plasma physics*. Department of University extention, the University of New England, 1964.

[2] E. Kuffel, W. S. Zaengl, and J. Kuffel. *High voltage engineeing: fundamentals*. Newness, 2000.

[3] D. J. Tedford. *High Voltage Technology*. Oxford University Press, 1968.

[4] M. Khalifa. *High Voltage Engineering: Theory and practice*. Marcel Dekker Inc., 1990.

[5] R. J. Gillespie, D. R. Eaton, D. A. Humphreys, and E. A. Robinson. *Atoms, molecules and reactions*. Prentice Hall, 1994.

[6] D. Kind and Herman Karner. *High Voltage insulation technology*. Friedrich Vieweg und Sohn, 1985.

[7] T. J. Gallagher and A. J. Pearmain. *High Voltage: Measurement and testing*. John Wiley and Sons, 1983.

[8] A. Beiser. *Concepts of modern Physics*. McGraw-Hill, fifth edition edition, 1995.

[9] R. A. Serway and R. J. Beichner. *Physics for scientists and Engineers*. Saunders College Publishing, fifth edition edition, 2000.

[10] *Introduction to laser safety*. NLC-CSIR, 2004.

[11] T. X. Phuoc. Laser spark ignition: experimental determination of laser-induced breakdown thresholds of combustion gases. Federal Energy Technology Centre, January 2000.

[12] Y. P. Raizer. *Laser-induced discharge phenomena*. Consultants Bureau, 1977.

[13] C. G. Morgan. Laser-induced breakdown of gases. *Reports on Progress in Physics*, (38):621–665, November 1975.

[14] P. X. Phuoc and C. M. White. Optical characterisation of the laser-induced spark in air. National Energy Technology Laboratory.

[15] R. A. Dougal, P. F. Williams, and A. H. Guenther. Breakdown process in laser-triggered switching. 4th IEEE International Pulsed Power Conference, 1983.

[16] N. J. West, D. M. Starfield, and I. R. Jandrell. Computer automation of a laser-triggered current impulse generator. South African Universities Power Engineering Conference 2004, 2003.

[17] L. L. Steinmetz. Laser-triggered spark gap. *Review of Scientific Instruments*, 39(6):904–909, June 1968.

[18] R. G. Adams, W. B. Moore, J. R. Woodworth, M. M. Dillon, F. Morgan, and K. J. Penn. Ultraviolet laser switching of a 5 megavolt multistage gas switch. 4th IEEE International Pulsed Power Conference, 1983.

[19] R. A Hamil and D. L. Smith. Laser triggered switch results from a frequency quadrupled nd:yag laser. 4th IEEE International Pulsed Power Conference.

[20] K. Ragaller. *Surges in high voltage networks*. Plenum Press, 1980.

[21] W. W. Lewis. *The protection of transmission lines against lightning*. John Wiley and sons, 1950.

[22] *IEC 60 High voltage test techniques, Part1: General definitions and test requirements*. SABS IEC, second edition 1989 edition, .

[23] *SABS IEC 61024 Protection of structures against lightning.* SABS IEC, 1993 edition, .

[24] C. Curry. *Geometrical Optics*. Edward Arnold and Co., 1956.

[25] T. W. Dakin, G. Luxa, G. Oppermann, Vigreaux, G. Wind, and H. Winkelnkemper. Breakdown of gases in uniform fields paschen curves for nitrogen, air and sulphur hexafluoride. *Journal of Physics D: Applied Physics*, 32:61–82.

Chapter 9

Appendix

9.1 Appendix A: Impulse generator model evaluation

The model was tested for a range of voltgaes from 1 kV to 20 kV. The following outputs (max. output voltage and percentage efficiency) were obtained:

Charging voltage: 1 kV
Max. Output voltage: 0.892 kV
Efficiency: 82.9% Plot of output voltage against time:

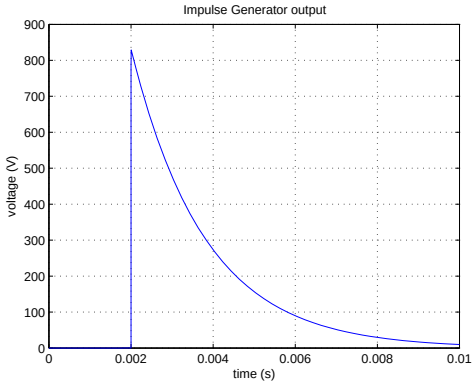


Figure 9.1: Impulse waveform for charging voltage of 1 kV

Charging voltage: 2 kV

Max. Output voltage: 1.658 kV

Efficiency: 82.9% Plot of output voltage against time:

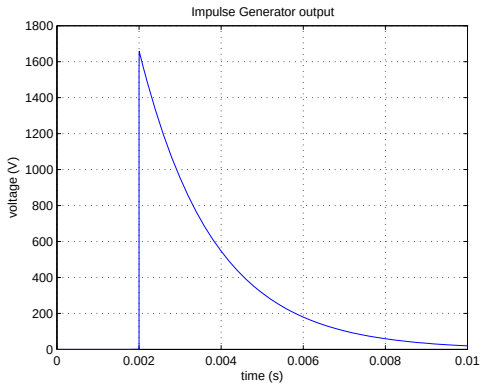


Figure 9.2: Impulse waveform for charging voltage of 2 kV

Charging voltage: 3 kV

Max. Output voltage: 2.486 kV

Efficiency: 82.8% Plot of output voltage against time:

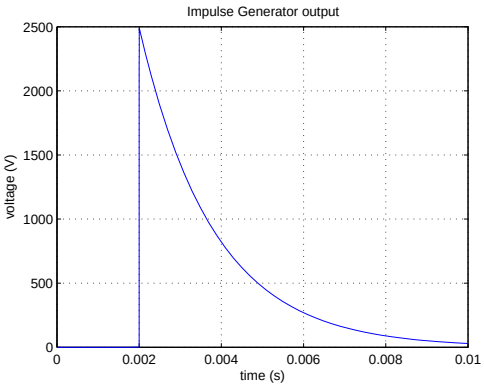


Figure 9.3: Impulse waveform for charging voltage of 3 kV

Charging voltage: 4 kV

Max. Output voltage: 3.315 kV

Efficiency: 82.8% Plot of output voltage against time:

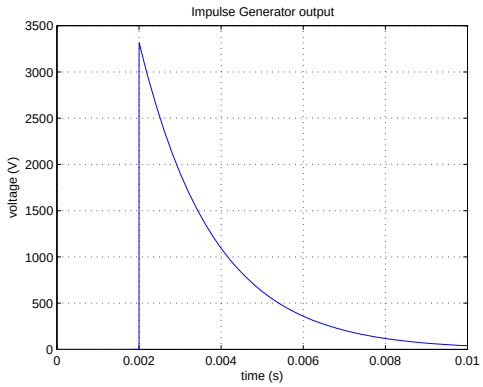


Figure 9.4: Impulse waveform for charging voltage of 4 kV

Charging voltage: 5 kV

Max. Output voltage: 4.144 kV

Efficiency: 82.8% Plot of output voltage against time:

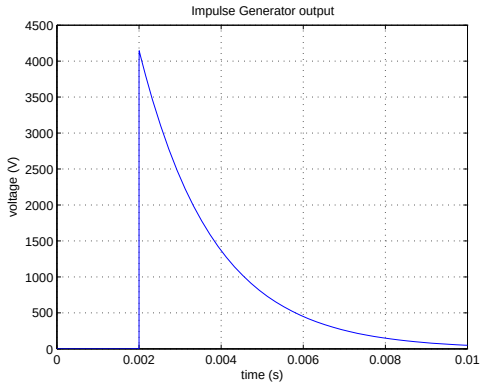


Figure 9.5: Impulse waveform for charging voltage of 5 kV

Charging voltage: 6 kV

Max. Output voltage: 4.973 kV

Efficiency: 82.8% Plot of output voltage against time:

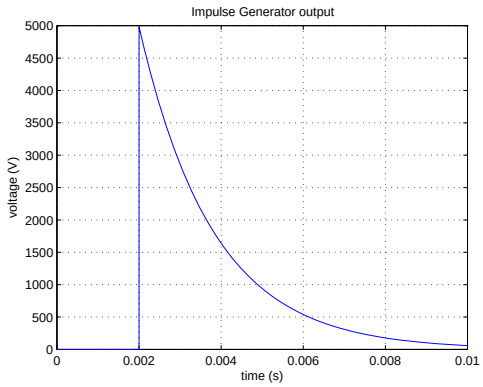


Figure 9.6: Impulse waveform for charging voltage of 6 kV

Charging voltage: 7 kV

Max. Output voltage: 5.802 kV

Efficiency: 82.8% Plot of output voltage against time:

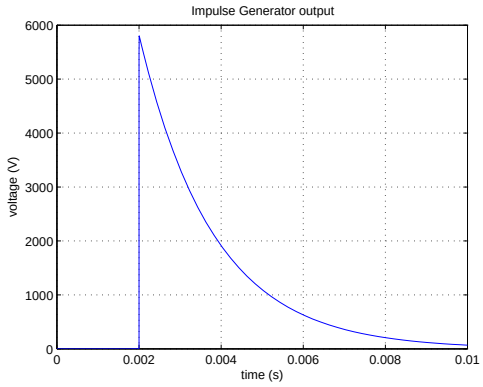


Figure 9.7: Impulse waveform for charging voltage of 7 kV

Charging voltage: 8 kV

Max. Output voltage 6.631 kV

Efficiency: 82.8% Plot of output voltage against time:

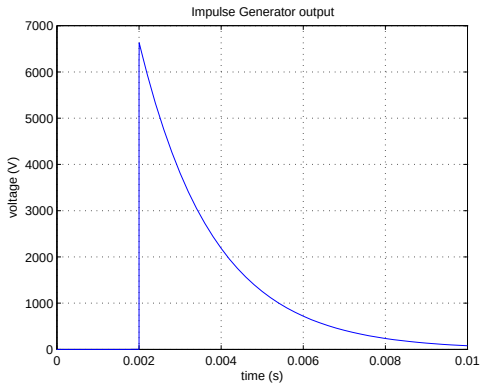


Figure 9.8: Impulse waveform for charging voltage of 8 kV

Charging voltage: 9 kV

Max. Output voltage: 7.460 kV

Efficiency: 82.8% Plot of output voltage against time:

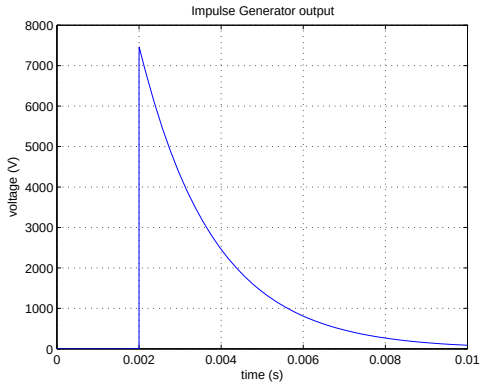


Figure 9.9: Impulse waveform for charging voltage of 9 kV

Charging voltage: 10 kV

Max. Output voltage: 8.288 kV

Efficiency: 82.8% Plot of output voltage against time:

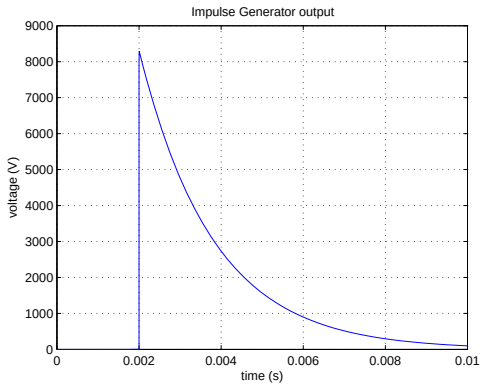


Figure 9.10: Impulse waveform for charging voltage of 10 kV

Charging voltage: 11 kV

Max. Output voltage: 9.116 kV

Efficiency: 82.8% Plot of output voltage against time:

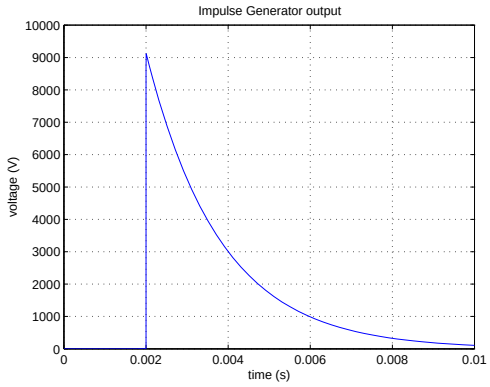


Figure 9.11: Impulse waveform for charging voltage of 11 kV

Charging voltage: 12 kV

Max. Output voltage: 9.945 kV

Efficiency: 82.8% Plot of output voltage against time:

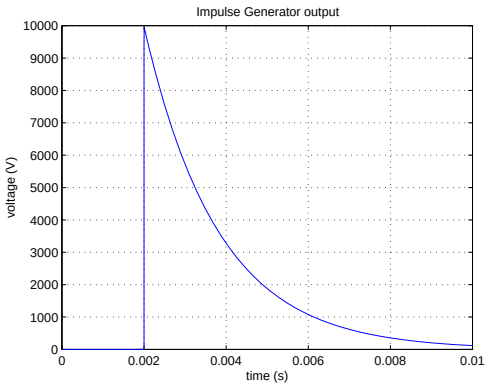


Figure 9.12: Impulse waveform for charging voltage of 12 kV

Charging voltage: 13 kV

Max. Output voltage: 10.774 kV

Efficiency: 82.8% Plot of output voltage against time:

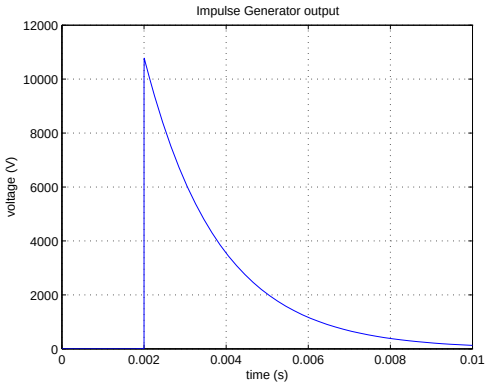


Figure 9.13: Impulse waveform for charging voltage of 13 kV

Charging voltage: 14 kV

Max. Output voltage: 11.604 kV

Efficiency: 82.8% Plot of output voltage against time:

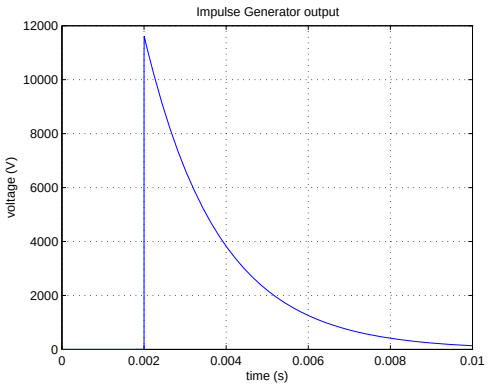


Figure 9.14: Impulse waveform for charging voltage of 14 kV

Charging voltage: 15 kV

Max. Output voltage: 12.433 kV

Efficiency: 82.8% Plot of output voltage against time:

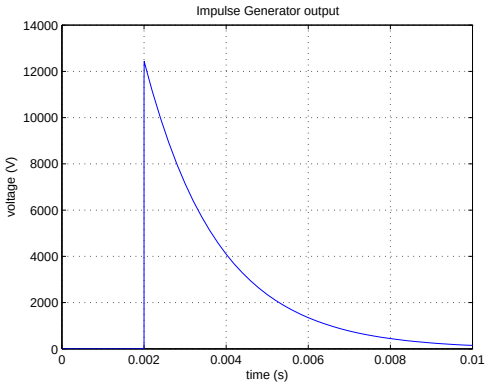


Figure 9.15: Impulse waveform for charging voltage of 15 kV

Charging voltage: 16 kV

Max. Output voltage: 13.262 kV

Efficiency: 82.8% Plot of output voltage against time:

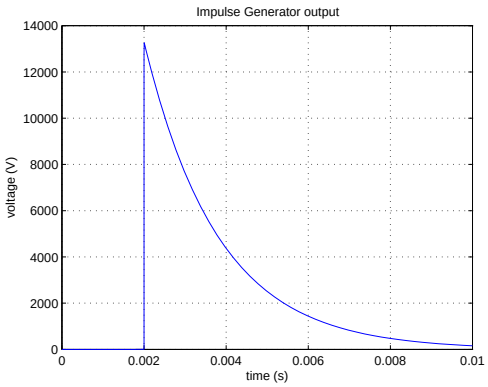


Figure 9.16: Impulse waveform for charging voltage of 16 kV

Charging voltage: 17 kV

Max. Output voltage: 14.091 kV

Efficiency: 82.8% Plot of output voltage against time:

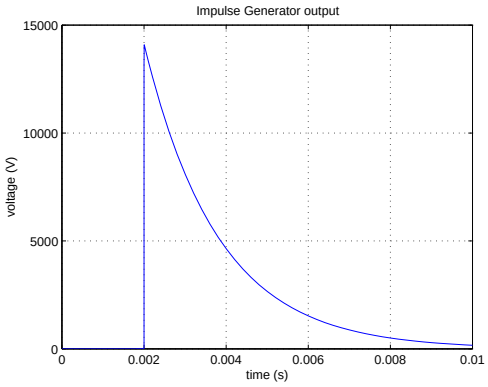


Figure 9.17: Impulse waveform for charging voltage of 17 kV

Charging voltage: 18 kV

Max. Output voltage: 14.920 kV

Efficiency: 82.8% Plot of output voltage against time:

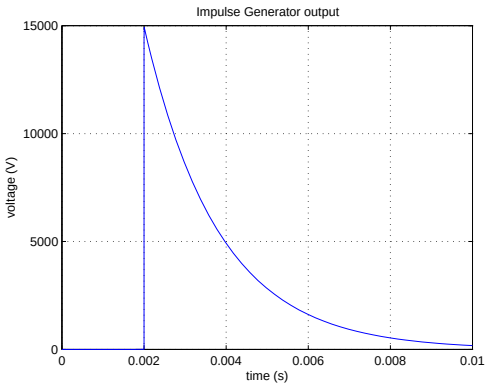


Figure 9.18: Impulse waveform for charging voltage of 18 kV

Charging voltage: 19 kV

Max. Output voltage: 15.474 kV

Efficiency: 82.8% Plot of output voltage against time:

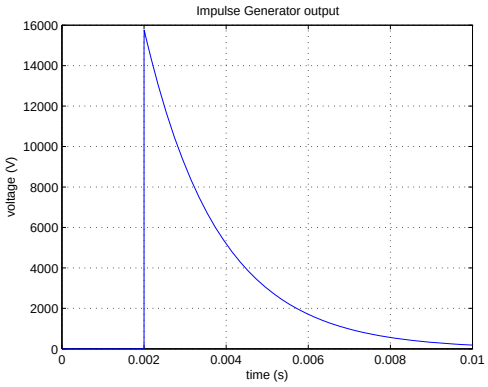


Figure 9.19: Impulse waveform for charging voltage of 19 kV

Charging voltage: 20 kV
Max. Output voltage: 16.575 kV
Efficiency: 82.8% Plot of output voltage against time:

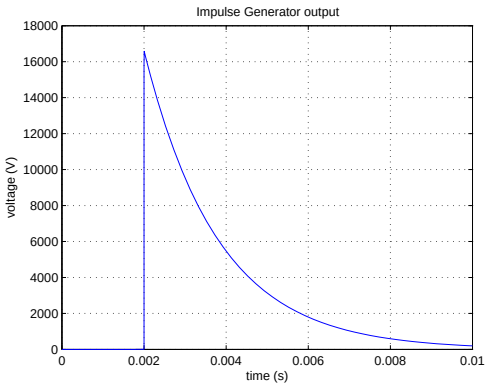


Figure 9.20: Impulse waveform for charging voltage of 20 kV

MATLAB code used to calculate the efficiency of the impulse generator.

```
%Matlab m-file used to calculate the efficiency of the
%mscvgenny3 simulink model of an impulse generator.
%The m-file evaluates the efficiency by finding the ratio of
%max. output voltage to charging voltage and converting it to
%a percentage.
%The m-file also converts the Simulink scope output into a
%Matlab plot.
%Just plotting the output
plot(t,Vop), grid, title('Voltage Impulse Output'),
             ylabel('Voltage (V)'), xlabel('Time (s)')

%Calculating efficiency
Voutput=round(max(Vop)) %The max output voltage
Vcharging=max(Vcharge)  %The max charging voltage
efficiency=(Voutput/Vcharging)*100
```

The MATLAB code used to evaluate the rise and fall time of the impulse generator waveforms can be seen below:

```
%Matlab m-file used to calculate the rise and fall time of
%the impulse waveform.
%Trise defined as time taken from 10% to 90% of signal.
%Tfall defined as time taken from 10% back to 50% of max.
%In other words: (time from 10% to 100%) + (time from 100% to 50%)
%Find max
ymax=max(Vop)
for i=1:128
    ratio=Vop(i,1)/ymax;
    if ratio == 1
        imax=i;
        break
    end
end
%Find 10%
for i=1:128
   ratio=Vop(i,1)/ymax;
   frac1=100*ratio;
   frac=round(frac1)/100;
    if frac == 0.1
        y10=Vop(i,1);
        i10=i;
        break
    end
end
%Find 50%
for i=80:128
   ratio=Vop(i,1)/ymax;
   frac1=10*ratio;
   frac=round(frac1)/10;
    if frac == 0.50
        y50=Vop(i,1);
        i50=i;
```

```
        break
    end
end
%Find 90%
for i=1:128
    ratio=Vop(i,1)/ymax;
    frac1=100*ratio;
    frac=round(frac1)/100;
    if frac == 0.9
        y90=Vop(i,1);
        i90=i;
        break
    end
end
%Find corresponding time values
%For 10%
t10=t(67,1);
%For 50%
t50=t(93,1);
%For 90%
t90=t(76,1);
%For max
tmax=t(82,1);

%Evaluate the rise and fall time
Trise=abs(t(67,1)-t(76,1));
Tfall=abs(t(67,1)-t(93,1));
%Time in microseconds
T1=Trise*1e6
T2=Tfall*1e6
```

9.2 Appendix B: Impulse generator experimental results

In this section, the experimentally obtained impulse generator output waveforms can be seen.

Charging voltage: 0.9 kV
Max. Output voltage: 0.736 kV
Efficiency: 81.8% Plot of output voltage against time:

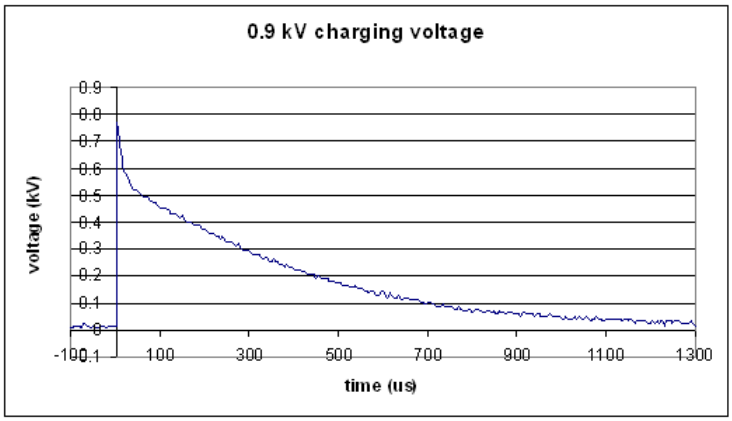


Figure 9.21: Experimentally obtained impulse waveform for 0.9 kV charging voltage

Charging voltage: 2.3 kV
Max. Output voltage: 1.88 kV
Efficiency: 81.7% Plot of output voltage against time:

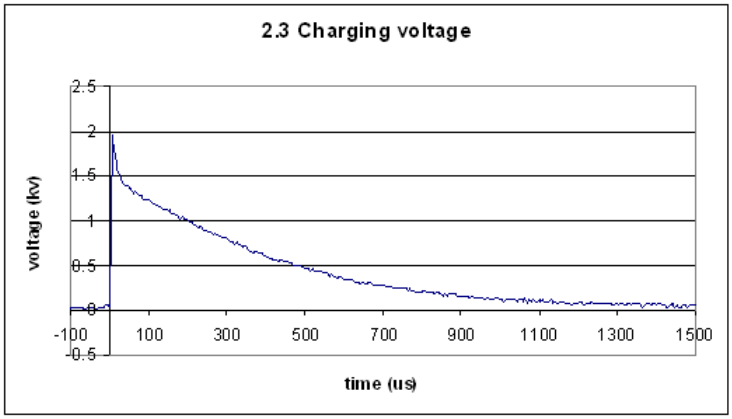


Figure 9.22: Experimentally obtained impulse waveform for 2.3 kV charging voltage

Charging voltage: 3 kV
Max. Output voltage: 2.44 kV
Efficiency: 81.3% Plot of output voltage against time:

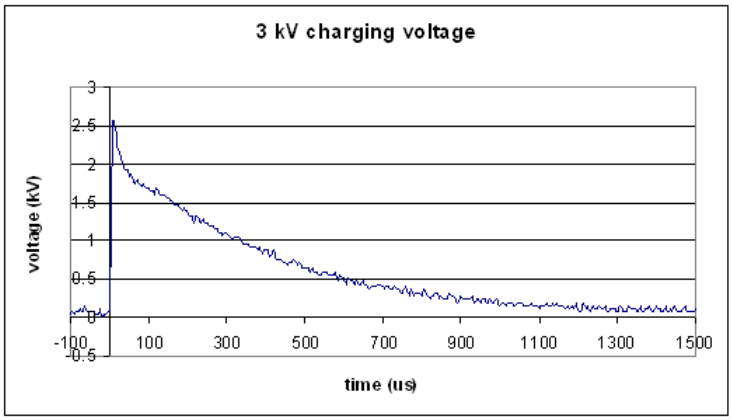


Figure 9.23: Experimentally obtained impulse waveform for 3 kV charging voltage

Charging voltage: 4.1 kV
Max. Output voltage: 3.36 kV
Efficiency: 82% Plot of output voltage against time:

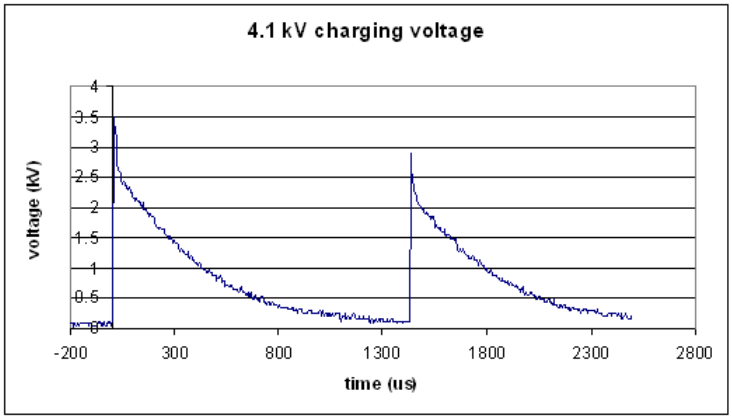


Figure 9.24: Experimentally obtained impulse waveform for 4.1 kV charging voltage

Charging voltage: 5.5 kV
Max. Output voltage: 4.56 kV
Efficiency: 82.9% Plot of output voltage against time:

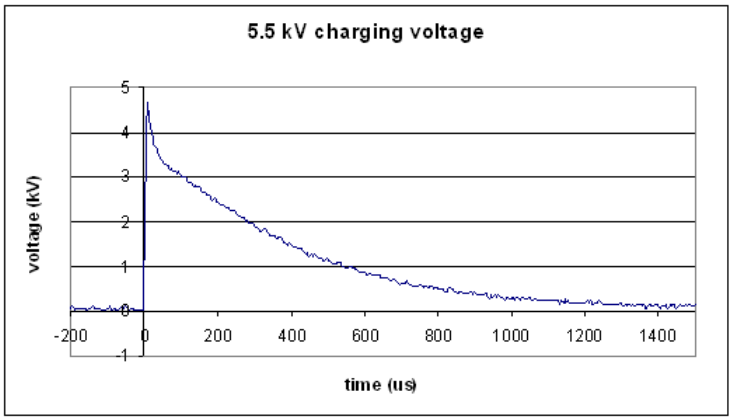


Figure 9.25: Experimentally obtained impulse waveform for 5.5 kV charging voltage

Charging voltage: 6 kV

Max. Output voltage: 4.76 kV

Efficiency: 79.3% Plot of output voltage against time:

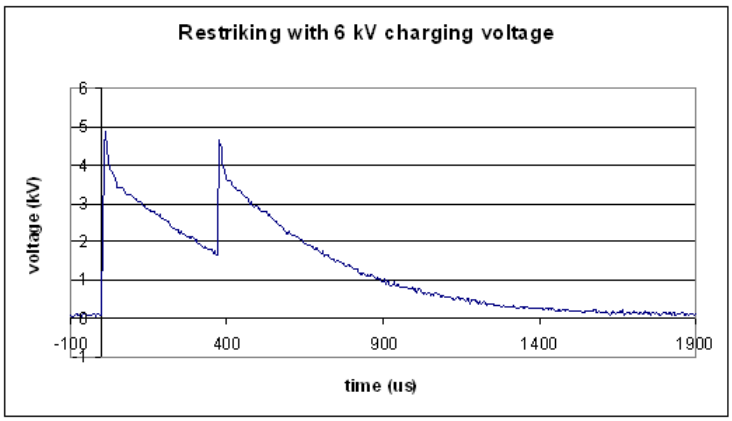


Figure 9.26: Experimentally obtained impulse waveform for 6 kV charging voltage

9.3 Appendix C: Pre-breakdown phenomena measurements

All measurements conducted in air at atmospheric pressure and temperature

Gap: 5mm		Gap: 5mm		Gap: 2.5 mm		Gap: 10 mm	
f=100 mm		f=100 mm		f=75 mm		f=100 mm	
E=200 mJ		E=160 mJ		E=141 mJ		E=193 mJ	
Voltage In	Voltage out	Voltage In	Voltage out	Voltage In	Voltage o	Voltage In	Voltage out
0.1	0	0.4	0.84	1	10.2	1	0
0.2	0	0.5	1.16	1.2	11.6	2	0.3
0.3	0	0.8	4.12	1.5	14	3	0.5
0.4	0.28	1	7.3	1.7	1190	4	1.1
0.5	0.2	1.2	9.72	1.8	1210	5	2
0.6	0.28	1.5	10.52	2	1430	6	2.1
0.7	0.52	2	17.8	2.3	1650	7	2.3
0.8	0.84	2.3	19.8	2.5	1810	8	3.5
0.9	1.08	3	27	3	2070	9	4.1
1	1.4	3.2	1960	4	3060	10	5.1
1.1	1.96			5	3660		
1.2	2.1			6	4060		
1.3	2.2			7	5140		
1.4	2.52						
1.5	2.84	Gap=2.5 mm		Gap=5 mm		Gap=10 mm	
1.6	2.92	f=75		f=75		f=75	
1.7	3.08	E=169		E=169		E=169	
1.8	3.32	Vin	Vout	Vin	Vout	Vin	Vout
1.9	4.2	0.1	17	0.5	0.6	1	0
2	4.4	0.2	18.2	0.6	1.72	2	0.32
2.1	4.68	0.3	25.4	0.7	2.04	3	1.28
2.2	4.84	0.4	276	0.8	2.84	4	1.92
2.3	4.92	0.5	300	0.9	3.24	5	2.96
2.4	5.08	0.6	375	1	4.76	6	4
2.5	5.56	0.7	428	1.5	6.12	7	4.72
2.6	5.96	0.8	500	2	7.96	8	5.68
2.7	6.12	1	700	2.5	10.68	9	8.4
2.8	6.28			2.7	12.36	9.1	7.44
2.9	7.16			3	15.2	9.4	7.28
3	7.48			3.1	16	9.7	7.52
3.2	8.84						
3.5	9.8						
3.6	72						
3.7	72						
3.8	1400						

Figure 9.27: Experimental data obtained for pre-breakdown phenomena

9.4 Appendix D: The engineering drawing

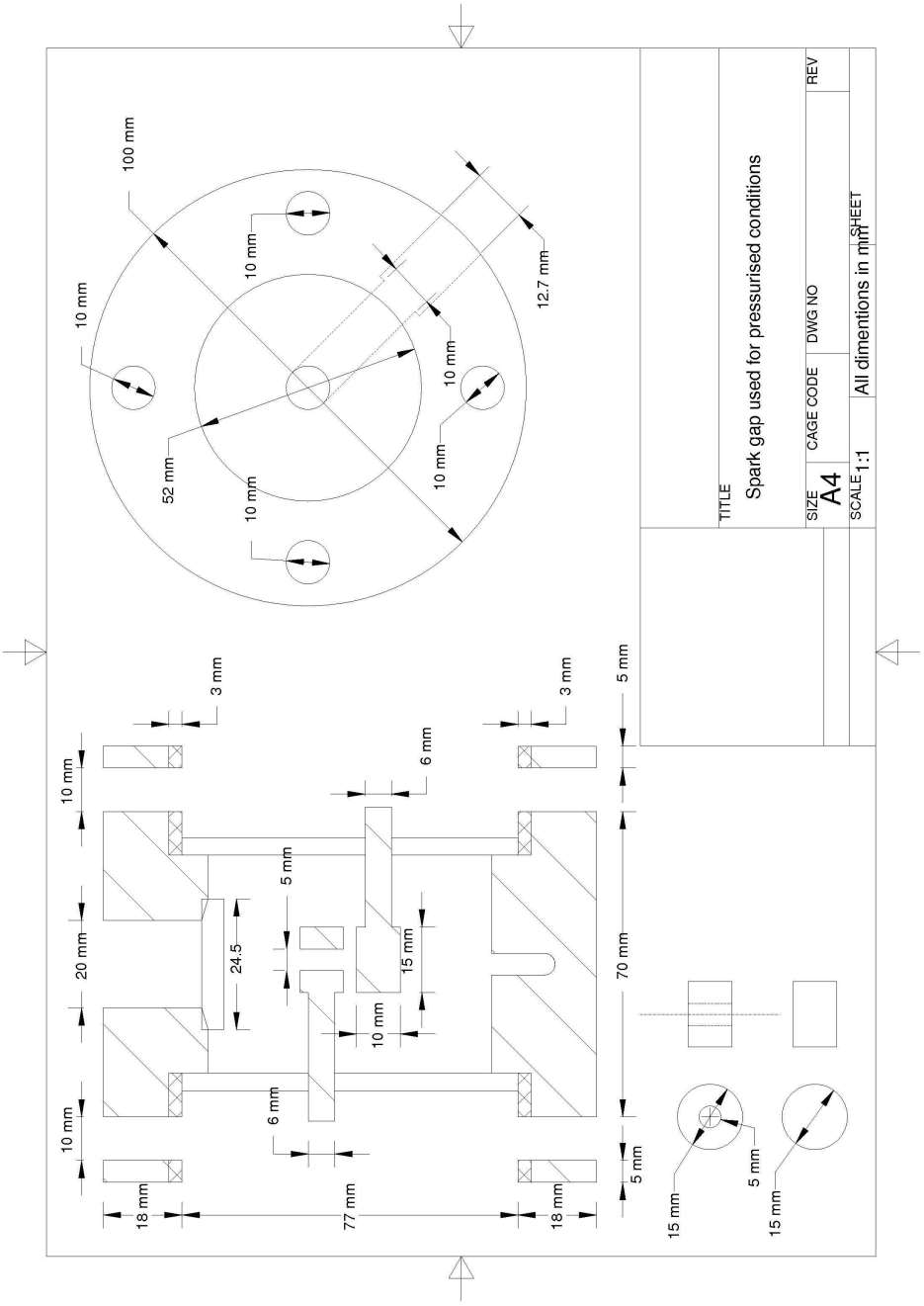


Figure 9.28: Experimental data obtained for pre-breakdown phenomena